IPPJ-AM-51

HIGH HEAT FLUX EXPERIMENTS ON C-C COMPOSITE MATERIALS BY HYDROGEN BEAM AT THE 10MW NEUTRAL BEAM INJECTION TEST STAND OF THE IPP NAGOYA

H.BOLT, A.MIYAHARA, T.KURODA, O.KANEKO
Y.KUBOTA, Y.OKA AND K.SAKURAI

INSTITUTE OF PLASMA PHYSICS
NAGOYA UNIVERSITY

NAGOYA, JAPAN

IPPJ-AM-51

HIGH HEAT FLUX EXPERIMENTS ON C-C COMPOSITE MATERIALS BY HYDROGEN BEAM AT THE 10MW NEUTRAL BEAM INJECTION TEST STAND OF THE IPP NAGOYA

H. Bolt*, A. Miyahara, T. Kuroda, O. Kaneko
Y. Kubota, Y. Oka and K. Sakurai

Institute of Plasma Physics, Nagoya University
Chikusa-ku, Nagoya 464, Japan

May 1987

*: on leave from Institute of Reactor Materials, Kernforschungsanlage
Juelich, P.B. 1913, D-5170 Juelich, FRG, Association EURATOM-KFA

Abstract

In order to meet the demand of the fusion community for a data base on the high heat flux behaviour of carbon - carbon composite materials (C-C composites), an experimental program on this issue had been initiated recently. A variety of 2-directional (2-d) and 4-directional (4-d) C-C composites were subjected to high heat flux pulses. The experimental device used in this study had been the 10MW Neutral Beam Injection Test Stand of the IPP Nagoya. In the experiments medium sized samples of about 30 mm x 30 mm surface were exposed to a hydrogen beam of about 1.4 MW power, an average power density of 100 MW/m^2 and pulse lengths between 69 ms and 315 ms. After the experiments no fatal cracks or fracture were detected on any of the samples. 2-d C-C composites showed very high erosion under heat flux incidence perpendicular to their weave orientation. The erosion on these materials greatly decreased with heat flux incidence parallel to the weave orientation. 4-d C-C composites showed moderate erosion in either direction. As one conclusion from the experiments very high heat fluxes under normal operation conditions on 2-d composites directed perpendicular to the weave orientation of material the (e.g. leading edges) should be avoided as high erosion has to be expected. From the viewpoint of resistance against cracks and fracture under high heat flux conditions all of the tested C-C composites have proved to be superior to graphites.

Contents

1. Introduction

Carbon materials have been increasingly applied as plasma facing materials of magnetic fusion devices during the last years. Graphite components are presently installed or to be installed in experimental devices like TFTR, JET, JT-60, TEXTOR, ASDEX, JIPP T2-U, and JFT-2M. As a result of the interest of the fusion community in the application of graphites a broad data base on these materials has been generated /1/. In addition to the continued strong interest on graphites, carbon - carbon composite materials (C-C composites) are attracting increasing attention as prospective plasma-facing materials for existing devices and, as option, for next generation devices (e.g. NET, FER). Main reasons for this interest are higher thermal shock stability and higher strength compared to graphites, as well as quasi-ductile behaviour and flexibility. Such advantages may lead to improved technological solutions in first wall engineering as heavy, complicated, and expensive (metal) backing structures could be reduced by applying self-supporting C-C composite structures. The higher thermal shock stability of C-C composites could drastically reduce concerns about component integrity under off-normal heat flux incidence, such as disruptions or neutral beam operation without plasma.

Though already applied in a few cases (e.g. JET NBI shine through armor, TEXTOR ALT-I pumplimiter head), the database on the applicability of C-C composites for fusion purposes is scarce. Especially in the crucial subject of the high heat flux behaviour of C-C composites until now only very limited knowledge exists (cf. 5.2). In order to meet the demand for an improved data base on the high heat flux behaviour of C-C composites the following study has been initiated.

In this study a variety of 2-directional (2-d) and 4-directional (4-d) C-C composites have been tested and compared comprehensively. The experimental facility used for the high heat flux experiments had been the 10 MW Neutral Beam Injection Test Stand of the Institute of Plasma Physics of Nagoya University. C-C composite samples were exposed to a hydrogen beam of high power density (about 100 MW/m^2) for short pulses (<315 ms). After the experiments the samples were examined under aspects of erosion and thermal shock stability.

2. Test stand

For the performance of high heat flux experiments on candidate first wall materials and full size first wall components the 10MW Neutral Beam Injection Test Stand at the IPP Nagoya /2-4/ had been modified. Figure 1 gives a schematic of the rebuilt test stand.

The ion source of the test stand produces hydrogen beams of up to 120 keV, 75 A and 1 s pulse duration with a gaussian shaped profile of the beam power density. The elongation factor of the oval shaped beam in vertical direction is roughly 2 and depends on the beam condition applied in experiments. For material tests the deflection coils of the test stand are not in operation thus ions and neutrals are striking the material test pieces at a distance of about 5 m from the ion source. Either a set of test pieces or full size first wall components can be inserted into the vacuum vessel by a lock system without breaking the vacuum of the vessel (about 10^{-4} Pa). A drive mechanism allows the test pieces to be vertically positioned in the H^+-beam. When operated without exposing test pieces to the beam, the beam is dumped into a calorimeter

which provides data for the calibration of high heat flux experiments. The repetition rate of the test stand is three to five minutes depending on the power supply mode. Table 1 gives a list of the test stand specifications for high heat flux materials experiments.

3. Experimental procedure

3.1 Materials, pretreatment and test procedure

2-d C-C composite materials used in the experiments were CC 139 C of Hitco Co., USA, KKarb 1200 of Kaiser Aerotech Co., USA, CF 322 of Schunk Kohlenstofftechnik, FRG, CX 20U of Toyo Tanso Co., Japan, and AMT and BMT of Mitsubishi Chemical Industries, Japan. 4-d C-C composite materials were FMI 3-3-3-3 and FMI 3-3-3-6 of Fiber Materials, Inc., USA.

For the experiments samples of a surface of about 30 mm x 30 mm (25 mm x 25 mm in the case of Schunk CF 322) with thicknesses varying from 6 mm to 11 mm were available for the experiments. As the profile of the beam power density is very broad, samples of this size placed in the beam center received a very homogeneous heat load over the whole sample surface (cf. 3.2). 2-d C-C composite samples which were to be subjected to heat flux incidence parallel to their weave orientation (||), had to be "sandwiched" together from small bars which were cut from C-C plates having the large surfaces in orientation of the weave as material of appropriate size was not available. All samples were cleaned in an ultrasonic bath with ethanol for three times five minutes each run. After each cleaning period the ethanol was exchanged.

The baking of the samples was performed at a temperature of $300^{o}C$ for 20 hours under a vacuum of 10^{-4} Pa. After the baking the samples were

stored under a vacuum of < 10 Pa until the experiment. In order to determine the influence of the baking procedure on the erosion process during the experiment, a few samples (Hitco CC 139 C and K-Karb 1200) were baked to 1400^{0} for 3 hours.

For the experiments a sample holder without cooling system was used. On the 15mm thick copper backing plate of the sample holder the sample was clamped at two edges by two pieces of graphite which were fixed to the copper backing plate by screws (see Fig. 2). The remaining portion of the copper sample holder was shielded against the beam by graphite dummy samples.

During the installation to the sample holder the samples were exposed to atmosphere for about 15 minutes. Afterwards they were kept in the back-up vacuum chamber of the lock system for the pump down of the vacuum. Before the experiment the gate valve to the NBI test vessel was opened and the samples inserted for beam exposure. After the experiment the sample holder was withdrawn and the samples removed, or kept for repeated exposure.

3.2 Beam calibration and beam parameters

For the beam calibration the calorimeter of the NBI Test Stand vacuum vessel was used. In this calorimeter 25 shielded thermocouples indicate the temperature rise during the beam impact. The horizontal and vertical spacing of the thermocouples in the plane perpendicular to the beam is 50 mm. Since the copper shielding of the thermocouples leads to the measurement of the temperature in the volume of the material, the recorded temperature is proportional to the energy dumped onto this

unit. Thus at a preset pulse length the temperature rise indicates the power density of the beam in this location.

After the conditioning of the ion source was finished and the beam conditions for high heat flux experiments - as indicated by the calorimeter values - were satisfied, the test pieces were positioned in the beam line so that during the next pulse the beam could hit the samples with beam conditions similar to the previously calibrated pulse onto the calorimeter with a variation of the beam power of less than 5%.

Figure 3 gives a calibration curve of the beam power density distribution of a pulse as it has been applied in the experiments. The peak power density of the pulses in the experiments varied from 93 MW/m^2 to 117 MW/m^2. Pulse lengths of 65 ms to 315 ms were obtained.

3.3 Post experiment treatment of the samples

After an experiment the sample was removed for further examination. All samples were examined visually and by SEM as well as the weight loss was measured by means of a microbalance. Aims of the observations were the clarification of the erosion process on composite materials under high heat flux conditions and the determination of the resistance to thermal shocks under disruption conditions.

3.4 Break down of the ion source and reconditioning

During experiments on C-C composites the ion source terminated operation after pulse lengths of 69 ms to 315 ms. This termination is due to arcing between the extraction grids of the ion source which seems to be caused by contamination of the grids. It is likely that the

contamination during the experiments occurs in the form of deposition of hydrocarbons reducing the field resistance against arcing or due to deposition of small carbon particles causing deformation of the electrical field between the grids.

After the experiments and the break down of the ion source caused by grid contamination extensive reconditioning of the ion sorce was needed to remove the contamination from the extraction grids and to reach experimental conditions again.

4. Results

A summary of the experimental results is given in Table 3.

4.1 Unexposed C-C composites

4.1.1 2-d C-C composite surfaces in weave orientation

Scanning electron micrographs of unexposed surfaces show that Hitco CC 139 C and Kaiser Aerotech KKarb 1200 are covered with a layer of an estimated thickness of several 10 µm (Figs. 4 a, b; 8 a, b). This layer seems to be a result from the densification process during the manufacturing of the materials. For observation of the weave structure below this coating and to test whether the coating is of influence on the experimental results, it was removed on several samples by grinding (see Table 2). After grinding the appearance of CC 139 C and KKarb 1200 surfaces is similar to the other 2-d C-C composites observed (Figs. 4 c, d; 8 c, d).

The surface structure of CC 139 C shows few voids which mainly occur

in areas where fibre strings of different directions intersect with each other (Fig. 4 c). The surface of KKarb 1200 shows far more voids, also occuring within fibre strings (Fig. 8 c, d). This may be caused by the stronger bending of the KKarb fibre strings during manufacturing as the weave is more closely knit compared to CC 139 C. In the case of Schunk CF 322 the surface appears to be homogeneous with few voids (Fig. 12 a) whereas Toyo Tanso CX-20U shows many voids within the fibre strings (Fig. 13 a). Although rather loosely knit, also Mitsubishi AMT shows the same kind of void, in this case of considerable length (Fig. 14 a). The random fibre orientation of Mitsubishi BMT results in large voids in areas of fibre intersection (Fig. 15 a). Large magnification micrographs reveal that spaces between single fibres are impregnated with filler from the densification process during production with close adhesion between fibres and filler (Figs. 4 d, 8 d, 12 b, 13 b, 14 b, 15 b).

4.1.2 2-d C-C composite surfaces perpendicular to weave orientation

The unexposed C-C surfaces perpendicular to the weave planes of CC 139 C, KKarb 1200, CF 322, and CX-20U appear all to be similar only with CC 139 C showing small numbers and CX-20U showing larger numbers of pore-like voids (Figs. 17 a, b, 18 a, b, 19 a, b, 20 a, b).

4.1.3 4-d C-C composites

The surface of FMI 3-3-3-3 does not show larger voids. Fibre strings in different directions seem to be well bound to each other as also obvious for the bonding of fibres to each other by the filler phase (Fig.22 a, b).

FMI 3-3-3-6 even before exposure to high heat fluxes shows weak adhesion of strings orientated in different directions with substantial cracks at the interfaces (Fig. 23 a).

4.2 C-C composites after exposure to high heat fluxes

4.2.1 2-d C-C composites subjected to heat fluxes perpendicular to the weave orientation

Generally the 2-d composites showed very high erosion under the applied heat loads of about 100 MW/m^2 with beam incidence perpendicular to the weave orientation (1). Because of this, the ion source of the test stand was rapidly contaminated by eroded species leading to early arcing in the source extraction grids and subsequently to termination of the pulse. The maximum pulse length obtained in the experiments described in this paragraph was 151 ms. The average pulse length of all experiments of this group was 103 ms (see Table 2).

As Hitco CC 139 C and Kaiser Aerotech KKarb 1200 could be tested more extensively because of better material supply, the results obtained on these materials are described more in detail. The behaviour of other materials is compared with CC 139 C and KKarb 1200 as reference.

Hitco CC 139 C (Figs. 5,6,7): The results of heat flux exposure of CC 139 C without removing the coating layer originating from the densification process (cf. 4.1.1) before the experiment is shown in Figure 5. The major part of the coating is eroded either by flaking off or by vaporization. In areas where the bare weave structure can be seen, the filler phase between the carbon fibres is preferentially eroded. The

fibres are thinned by vaporization under the incident heat flux (Fig. 5 b). The average weight loss amounted to 12.4 mg per shot of an average pulse length of 128 ms.

The repeated heat flux exposure of one sample through five subsequent pulses resulted in an overall weight loss of 51 mg which makes an average loss of 10.2 mg per pulse with an average pulse length of 121 ms. Thus the erosion yield stays almost constant under repeated pulses leading to the conclusion that the surface layer on the material is not responsible for the very high erosion of this material in the experiments. SEM micrographs of the sample surface show that the surface layer almost completely disappeared, and that the weave material has been subjected to severe erosion (Fig. 6 a, b).

Furtherly samples from which the coating was removed by grinding before the experiment were exposed to the beam. Pulse lengths and weight losses are comparable to the results obtained before. Figure 7 b shows an erosion structure of the fibres similar to that of Figure 5 b, a sample irradiated with coating.

None of the sample surfaces shows cracks which may be attributed to the thermal shocks. The voids on the surface of unirradiated material (cf. 4.1.1) do not serve as sites for crack initiation.

Kaiser Aerotech KKarb 1200 (Figs. 9, 10): Compared to CC 139 C the pulse duration which could be obtained before termination of the pulse due to contamination of the ion source was significantly shorter with KKarb 1200 (average pulse length: 86 ms). Even then the weight losses during

these pulses were larger than those obtained on CC 139 C samples (average weight loss per pulse: 12.9 mg). Thus the erosion of KKarb 1200 is more severe than that of CC 139 C.

On samples subjected to irradiation with coating layers (cf. 4.1.1), these layers are almost completely removed in the experiment allowing exposure of the bare weaves to the ion beam (Fig. 9 a). Filler phase and carbon fibres are homogeneously eroded at the same time (Fig. 9 b). The experimental results with respect to pulse length and erosion do not improve with a removal of the surface coating before the experiment. Numerous pre-existent voids on the surface of KKarb 1200 (Fig. 8c) do not serve as sites for crack initiation under thermal shocks.

Schunk CF 322 (Figs. 11 a, 12): The material was eroded homogeneously during beam exposure (Fig. 12 c, d). Taking the smaller sample size into account, the erosion of CF 322 is gradually less than the erosion of KKarb 1200 (see Table 2). No cracks on the sample surface were observed.

Toyo Tanso CX-20U (Figs. 11 b, 13): The filler between the carbon fibres is preferentially eroded during the beam pulse (Fig. 13 d). Although the surface of this material shows many voids in the weave plane, no cracks were initiated from these voids (Fig. 13 c).

Mitsubishi Chem. Ind. AMT (Figs. 11 c, 14): Also on this material the filler phase is preferentially eroded leaving carbon fibres bare (Fig. 14 d). The weight loss of AMT in the experiment is less than the weight losses of KKarb 1200 samples and is comparable to the performance of CC 139 C (weight loss of 7.4 mg during a pulse of 107 ms). Although already

long voids between fibres exist before irradiation, no cracks were initiated from these sites during the experiment.

Mitsubishi Chem. Ind. BMT (Figs. 11 d, 15): The erosion structure of this material and the sensitivity to erosion is comparable to the before mentioned AMT grade (weight loss of 11.3 mg during a pulse of 120 ms). No cracking is observed.

In order to determine whether the pretreatment of the samples is of influence on the erosion behaviour several CC 139 C and KKarb 1200 samples were outgassed to 1400°C for 3 hours thus significantly exceeding the standard pretreatment temperature of 300°C. In the experiments no major difference between the erosion behaviour of these two types of samples was observed (see Table 2).

The results obtained in the experiments on 2-d C-C composites with heat loads perpendicular to the weave direction (⊥) can be summarized as follows:

- All materials tested showed very high erosion.
- A coating of C-C surfaces originating from the manufacturing process does not significantly influence the erosion behaviour.
- The weight loss per pulse under repeated heat fluxes to the same sample stays approximately constant in subsequent pulses.
- An annealing of the samples before the experiment to 1400°C does not influence the erosion behaviour compared to a treatment at 300°C.
- No cracks on the samples were observed which might have been caused by the thermal shocks.

4.2.2 2-d C-C composites subjected to heat fluxes parallel to the weave orientation

In general beam pulses in direction parallel to the weave orientation of the material (∥) were sustained longer than in the experiments with heat fluxes in perpendicular direction (⊥) described above. The longer pulses indicate a substantially reduced erosion as the contamination of the ion source of the test stand takes longer time which leads to a later termination of the pulse. The average pulse length in the experiments of this group was 215 ms.

Hitco CC 139 C (Figs. 16 a, 17): Thermal loads on CC 139 C samples did not lead to extensive damage. Several microcracks were initiated from small voids in the weave strings orientated in beam direction (Fig. 17 c, arrow). These cracks are deflected or stopped when reaching a fibre string of different orientation. Thus further crack propagation is prevented and the microcracks cannot grow to a critical size. Although the fibres on the sample surface are orientated perpendicular and parallel to beam incidence, the erosion attack to the material appears homogeneous. The erosion pattern of the fibres orientated perpendicular to beam incidence is the same like the erosion pattern of samples exposed on surfaces oriented with the weave plane (⊥) (compare Fig. 5 b and Fig. 17 d).

The weight loss recorded in one experiment on CC 139 C amounted to 11 mg during a pulse of 208 ms duration with a power density of 117 MW/m^2.

Kaiser Aerotech KKarb 1200 (Figs. 16 b, 18): During the thermal shock several cracks occured in the areas of fibre orientation in direction of

beam incidence (Fig. 18 c). Like in CC 139 C these cracks are deflected and stopped at the interfaces to fibre strings of different orientation. The erosion pattern of KKarb 1200 is similar to the CC 139 C material described before. The recorded weight loss during one experiment was 19.1 mg for a pulse length of 164 ms and a power density of 102 MW/m^2. Although this indicates a reduced erosion compared to the erosion under heat fluxes perpendicular to the weave orientation ($\perp$) of KKarb 1200 samples, the weight loss is well above that of CC 139 C.

Schunk CF 322 (Figs. 16 c, 19): No cracks were observed with this material. Figure 19 c indicates that fibre strings in orientation perpendicular to the incident heat flux are stronger eroded than those orientated with the heat flux direction. The pulse length obtained in the experiment with this material is comparable to the pulse length obtained with CC 139 C (277 ms at a power density of 99 MW/m^2).

Toyo Tanso CX-20U (Figs. 16 d, 20): Starting from preexistent voids several microcracks occured which were stopped at the interfaces with fibre strings of different orientation (Fig. 20 c, arrow). Under higher magnification only slight traces of erosion can be detected as heat flux and pulse length during this experiment were moderate (96 MW/m^2 for 170 ms).

The results obtained on 2-d C-C composites under heat flux incidence parallel to the weave orientation ($\parallel$) can be summarized as follows:

- Cracks may occur in areas of fibre strings orientated in direction of the heat flux (CC 139 C, KKarb 1200, CX-20U). This cracks are stopped at the interfaces to fiber strings of different orientation and thus they do not become critical.

- Erosion under heat fluxes in this direction (∥) is greatly reduced compared to heat fluxes on 2-d C-C composites perpendicular to the weave orientation (⊥) (cf. 4.2.1).

4.2.3 4-d C-C composites

The grades used in the experiments (FMI 3-3-3-3 and FMI 3-3-3-6) were subjected to heat fluxes in two different directions. The results obtained did not show dependence on the direction of the heat load.

FMI 3-3-3-3 (Figs. 21 a, b, 22): Caused by the heat load cracks occured (Fig. 22 c). These cracks mainly propagated around fibre strings orientated with the direction of the beam incidence (compare Fig. 21 a and 22 c). Also cracks occured parallel to fibre strings orientated with the direction of beam incidence. No propagation across the interface between fibre strings of different orientation was found.

Erosion of the sample surface during the experiment was homogeneous with weight losses well below those recorded for 2-d C-C composites under beam incidence perpendicular to weave orientation (average weight loss 6.2 mg at an average pulse duration of 204 ms).

FMI 3-3-3-6 (Figs. 21 c, d, 23): An increase of the extensive preexistent cracking was not observed (cf. 4.1.3). Like with FMI 3-3-3-3 the erosion of the sample surface appears homogeneous. Weight losses during pulses of up to 315 ms were very moderate (average weight loss 10.1 mg at an average pulse duration of 271 ms). The erosion behaviour of FMI 3-3-3-3 and FMI 3-3-3-6 is comparable.

The results on 4-d C-C composites can be summarized as follows:

- If not already preexistent, considerable cracking occurs during high heat flux incidence. Cracks do not propagate across interfaces between fibre strings.
- Erosion of these materials is very moderate.

5. Discussion

5.1 Erosion of C-C composites under high heat fluxes

For a comprehensive evaluation of the experimental results on C-C composite materials the weight loss in the experiment was correlated to a heat flux parameter F as shown in Figure 24. The heat flux parameter F

$$F = \frac{P}{A} \cdot \sqrt{t} \qquad (1)$$

with: P/A: power density in MW/m^2

t: duration of the heat flux in s

was chosen to combine the factors power density and duration of the heat load in one parameter which is in accord with the process of one-dimensional surface heating. In this case the rise of the surface temperature is given as

$$\Delta T = \frac{P}{A} \cdot \sqrt{t} \, \frac{2}{\sqrt{\pi \rho c_p k}} \qquad (2)\ /5\text{-}7/$$

with: ρ: density of the material

c_p: specific heat

k: thermal conductivity.

This approximation is valid for energy deposition times shorter than the thermal diffusion time t_d of the sample

$$t_d = \frac{d^2 \pi \rho c_p}{4k} \qquad (3)\ /6,7/$$

with: d: thickness of the sample perpendicular to the incidence of the heat flux

and for temperatures where significant evaporation does not occur. Throughout the experiments the pulse lengths were shorter than the thermal diffusion time t_d of the samples. As in the experiments the heating conditions were almost one-dimensional in the area of the sample (broad energy density distribution profile of the beam, Fig. 3), the heat flux parameter F is a parameter in close relation to the thermal reaction of the sample. This parameter allows to compare the erosion results of the experiments, although the pulse lengths varied in between 69 and 315 ms. Figure 24 shows the experimental results obtained with 2-d and 4-d C-C composites. For comparison also results obtained on five different grades of graphite (POCO AXF-5Q, Union Carbide ATJ, Carbone Lorraine CL 5890 PT, Toyo Tanso IG 110, and Ibiden ETP-10) which were tested as limiter tile models are included. The results on graphite are to be discussed in detail at another place.

Figure 24 shows that three groups of materials can be clearly distinguished: 2-d C-C composites eroded under heat fluxes perpendicular to the weave orientation ($\perp$), graphites, and 4-d C-C composites. Two samples of the 2-d C-C composites subjected to heat fluxes parallel to their weave orientation ($\parallel$) (Hitco CC 139 C and Kaiser Aerotech KKarb 1200) are also indicated.

It can be seen that all 2-d C-C composites, independent of the grade, show considerable erosion already at comparatatively low heat fluxes, if the heat flux is directed perpendicular to the weave orientation (⊥). With heat flux incidence parallel to the weave orientation of 2-d samples the erosion behaviour is improved which is especially obvious in the case of the Hitco CC 139 C sample.

Erosion occurs on graphites at higher heat fluxes with weight losses rapidly increasing with heat flux. The lowest weight losses as function of the incident heat fluxes occured on 4-d C-C composites showing an erosion behaviour even superior to graphites.

Among 2-d C-C composites differences in the erosion behaviour were observed. Results indicate that Hitco CC 139 C and the Mitsubishi grades AMT and BMT show gradually less erosion than Kaiser Aerotech KKarb 1200 and Schunk CF 322.

The reason for the in general very unfavourable erosion behaviour of 2-d C-C composites with heat flux incidence perpendicular to the weave orientation (⊥) may be explained by the significantly lower thermal conductivity across the weave planes of these materials compared to the thermal conductivity along the weave planes which is in the order of the thermal conductivity of graphites /8/. Thus the removal of heat generated on a surface in weave orientation is slow as the thermal conductivity across the weave planes is rather low. As a result, under heat loads the temperature of such a surface rapidly rises (eq. 2) and subsequently significant amounts of the incident heat flux are consumed by vaporization leading to large weight losses even under heat fluxes

where graphites and 4-d C-C composites do not yet show any erosion (Fig. 24). Accordingly 2-d C-C composites show less erosion when thermally loaded in the other direction (||).

Damage by cracking under the applied heat loads was not observed on any 2-d C-C sample with heat flux incidence perpendicular to the weave plane orientation ($\perp$). Heat fluxes on surfaces parallel to the weave plane orientation (||) caused cracking on some materials (CC 139 C, KKarb 1200, CX-20U) which is assumed to be uncritical as the cracks are stopped at the interfaces with fibre strings of different orientation (cf. 4.2.2). Thus cracking, compared to erosion, appears to be a minor concern in the application of 2-d C-C composites as high heat flux components. The cracking observed on one 4-d composite material (FMI 3-3-3-3) and the pronounced preexistent cracks on the FMI 3-3-3-6 material seem to be uncritical as also in these materials cracks are stopped at interfaces with fiber strings of different orientation.

Thus, in a general comparison with the high heat flux behaviour of graphites /9-15/ the occurance of cracks is far less critical with C-C composites as either they are not initiated or initiated cracks are immediately stopped by the structure of the composite material.

5.2 Comparison of the experimental results with results of other studies

The results of a feasibility study carried out on C-C composites by use of the Neutral Beam Injection Test Stand of JET /16, 17/ are in general agreement with the experimental results of this study. At JET considerable weight losses were observed when exposing 2-d C-C composite

samples to heat fluxes perpendicular to the weave plane ($\perp$) (grades of Dunlop and Carbone Lorraine). No cracking was observed on either of the samples.

In the frame of a study on the high heat flux behaviour of graphites performed at KFA Juelich also one C-C composite material (Dunlop E 5923) was tested by electron beam heating /18, 19/. Although the amount of eroded material did not drastically vary from those of graphites tested, tests of the material with heat fluxes perpendicular to the weave orientation of the sample ($\perp$) resulted in about threefold erosion compared to heat fluxes incident parallel to the weave orientation ($\parallel$).

A study carried out at Sandia National Laboratories, Albuquerque, /9, 10/ is in agreement with the results of this study insofar, as also there 2-d C-C composites showed considerably higher erosion compared to the graphite materials tested in the same program. On the other hand side electron beam irradiation led to very high weight loss on a FMI 4-d composite during a heat pulse of 100 MW/m^2 for 1 s. During the experiment intense particle emission was observed which might be responsible for a major portion of the weight loss. In order to determine the causes for this discrepancy further experiments with 4-d C-C composites are necessary as the data basis for these materials is obviously not yet sufficient.

5.3 Implications of the experimental results for the application of C-C composites as in-vessel components

Compared to graphites which were tested in a previous study /15/ C-C composites are superior in terms of cracking and fracture as crack propagation is stopped at the interfaces of fibre strings of different orientation. However the application of 2-d C-C composite materials as in-vessel components needs careful consideration as the thermal properties of these materials are highly dependent on the orientation. Low thermal conductivity in direction across the weave planes leads to high surface temperatures and thus to high erosion under heat fluxes incident in this direction ($\perp$). Because of this, the application of 2-d C-C composites facing heat flux in this direction should be restricted to regions which do not receive high heat fluxes under normal operation conditions. When applied as components receiving high heat fluxes in direction perpendicular to the weave planes ($\perp$) high erosion and thus a very limited lifetime has to be taken into consideration.

The advantages of the excellent thermal shock properties of 2-d C-C composites in terms of resistance against fracture can be taken by using these materials as armor of wall portions which only receive high heat fluxes under off-normal conditions (e.g. disruptions, neutral beam strike during NBI without plasma) or as wall armor against mechanical impact (wall portions opposite to pellet injection ports). High heat fluxes on this armor during off-normal operation would cause high erosion which is acceptable when the frequency of these events is low.

In the application of 2-d C-C composite components receiving high heat

fluxes under normal operation conditions the heat flux incidence should be parallel to the weave orientation of the material (||), that is in direction of high thermal conductivity. In this case under high heat fluxes an erosion behaviour similar to that of graphites without the disadvantage of fatal failure due to fracture of the component can be expected. The major disadvantage in this way of 2-d C-C composite application lies in the availability of these materials as panels with the large area surfaces in orientation of the weave plane. Thus an application of 2-d composites for large area high heat flux components makes a "sandwiching" of rather thin panels necessary which were cut from the original large area panels and then turned into the direction of high thermal conductivity. In this case a major portion of the technological advantages of 2-d C-C composite would be lost.

A possible solution might be the application of 4-d C-C composites for such components. As presently the erosion behaviour of these materials is contradictory in different studies (cf. 5.2) further work for a definite answer is necessary.

6. Conclusions

High heat flux experiments by hydrogen beam on a variety of C-C composite materials were carried out by use of the Neutral Beam Injection Test Stand of the IPP Nagoya. Heat loads of about 100 MW/m^2 for durations of 69 ms to 315 ms were applied to 2-d C-C composites, namely Hitco CC 139 C, Kaiser Aerotech KKarb 1200, Schunk CF 322, Toyo Tanso CX-20U, Mitsubishi Chem. Ind. AMT and BMT and 4-d C-C composites, namely FMI 3-3-3-3 and FMI 3-3-3-6. The following conclusions from the experimental results can be drawn:

a) Severe cracking leading to fracture of C-C composite tiles did not occur as crack propagation is stopped at the interfaces of fibre strings of different orientation.

b) Delamination on samples in the experiments was not observed.

c) Severe erosion occured on 2-d C-C composite samples under heat fluxes incident perpendicular to the weave orientation ( ) which may be caused by the low thermal conductivity of the materials in this direction.

d) A coating layer on CC 139 C and KKarb 1200 samples originating from the densification process during production does not alter the experimental results with regard to erosion and cracking.

e) Baking to higher temperatures than 300°C (1400° for 3 hours) prior to the experiment does not lead to improved results in terms of erosion.

f) Heat flux incidence on 2-d C-C composite samples parallel to the weave orientation ( ) leads to significantly reduced erosion on the materials compared to c).

g) 4-d C-C composites show less erosion than 2-d composites, independent of the direction of the heat flux but cracks are more frequent.

Acknowledgement

The assistance of Dr. C. D. Croessmann, Sandia National Laboratories, Albuquerque, during the course of the work is greatly acknowledged.

References

/1/ Contributions to the "Japan - US Workshop on Plasma Material Interaction / High Heat Flux Data Needs for the Next Step Ignition and Steady State Devices", IPP Nagoya, Jan. 26 - 30, 1987, to be published

/2/ O. Kaneko, Y. Oka, K. Sakurai, T. Kuroda, Proc. 10th Symp. on Fusion Engineering, Philadelphia (1983)

/3/ Y. Oka, O. Kaneko, K.Sakurai, T. Kuroda, K. Hayashi, K. Masuda, Y. Samada, Proc. 13th Symp. on Fusion Technology, Varese (1984)

/4/ Y. Oka, O. Kaneko, K.Sakurai, T. Kuroda, Nucl. Eng. Design/Fusion 4 (1987) 387

/5/ J. P. Holman, Heat Transfer, McGraw Hill, New York (1986)

/6/ R. de Coninck, A. Gijs, M. Snijkers, Rev. int. hautes Tempér. Réfract., Fr. 16 (1979) 294

/7/ R. Behrisch, J. Nucl. Mater. 93+94 (1980) 498

/8/ Kaiser Aerotech Co., product information on KKarb materials and Schunk Kohlenstofftechnik, product information on CF-materials

/9/ J. Bohdansky, C. D. Croessmann, J. Linke, J. M. McDonald, D. H. Morse, A. E. Pontau, R. D. Watson, J. B. Whitley, D. M. Goebel, J. Hirooka, O. Leung, R. W. Conn, J. Roth, W. Ottenberger, H. E. Kotzlowski, to be published in Nucl. Instr. Meth. B

/10/ J. Bohdansky, C. D. Croessmann, J. Linke, Proc. 14th Symp. on Fusion Technology, Avignon (1986), to be published

/11/ C. D. Croessmann, Ph.D. Thesis, University of Wisconsin (1986)

/12/ K. Ioki, M. Nishikawa, I. Tatsumi, T. Uchikawa, M. Fujiwara, J. Nucl. Sci. Technol. 22 (1985) 529

/13/ K. Ioki, M. Yamada, N. Nishikawa, T. Uchikawa, M. Onozuka, H. Yamao, to be published in Fusion Eng. Design 5 (1987)

/14/ M. Shibui, J. Ohmori, T. Kuroda, Proc. 14th Symp. on Fusion Technology, Avignon (1986), to be published

/15/ H. Bolt, C. D. Croessmann, A. Miyahara, T. Kuroda, Y. Oka, K. Sakurai, "Japan - US Workshop on Plasma Material Interaction / High Heat Flux Data Needs for the Next Step Ignition and Steady State Devices", IPP Nagoya, Jan. 26 - 30, 1987, to be published

/16/ K. J. Dietz, private communication (1987)

/17/ H. Brinkschulte, "2nd Workshop on Graphite for Fusion Applications", KFA Juelich, March 17, 1986

/18/ J. Linke, W. Delle, H. Hoven, E. Wallura, private communication (1986)

/19/ W. Delle, "1st Workshop on Graphite for fusion applications", KFA Juelich, Nov. 21, 1985

NBI - Test Stand

specifications for high heat flux experiments on C-C composites:

H^+-ion beam:	120 keV, 75 A
beam divergence:	0.55^o (horizontal axis) 1.2^o (vertical axis)
electrode size:	150mm x 600mm
focal point:	9500mm
heat load on test pieces:	$\sim$ 100 MW/m^2
pulse length:	$<$ 1 s
size of components to be tested:	$<$150mm x 400mm

Table 1: Test stand specifications for high heat flux experiments on C-C composites

sample	preparation	direction of beam incidence	shot #	pulse length (ms)	power density (MW/m^2)	weight loss (mg)	remark
CC139C		⊥	29750	132	95	15.7	
CC139C		⊥	32422	151	95	8.7	
CC139C		⊥	-32665	101	105	12.9	
CC139C	1400°C, 3h	⊥	1244	139	97		5 shots
		⊥	1375	107	100		on one
		⊥	1377	113	103		sample
		⊥	1397	107	99		
		⊥	1416	139	97	Σ50.1	
CC139C	srf. ground 1400°C, 3h	⊥	1462	113	97	7.0	
CC139C	srf.ground 1400°C, 3h	⊥	1586	145	97	9.7	
K-Karb		⊥	29769	69	110		2 shots
		⊥	29809	76	105	Σ27.3	on one sample
K-Karb		⊥	32183	145	93	14.3	
K-Karb		⊥	-32645	69	102		2 shots
		⊥	3	69	101	Σ21.5	on one sample
K-Karb	srf. ground 1400°C, 3h	⊥	1534	76	100	14.0	
K-Karb	srf. ground 1400°C, 3h	⊥	1631	95	99	13.1	
CF 322		⊥	29980	76	97	4.8	$25^2 mm^2$
CF 322		⊥	32129	76	96	4.3	$25^2 mm^2$
CF 322		⊥	32505	69	102	7.8	$25^2 mm^2$
CX-20U		⊥	30294	76	101		
AMT		⊥	29996	107	99	7.4	
BMT		⊥	30280	120	103	11.3	

Table 2, continued

sample	preparation	direction of beam incidence	shot #	pulse length (ms)	power density (MW/m^2)	weight loss (mg)	remark
CC139C		∥	31490	290	100		
CC139C		∥	32579	208	117	11.0	
K-Karb		∥	31529	183	99		
K-Karb		∥	32627	164	102	19.1	
CF 322		∥	32026	277	99		
CX-20U		∥	32093	170	96		
FMI 3333		1st dir.	30335	151	104	0.9	
FMI 3333		1st dir.	32678	258	102	10.0	
FMI 3333		2nd dir.	31207	202	102	7.7	
FMI 3336		1st dir.	31140	315	108	16.0	
FMI 3336		1st dir.	32738	183	100	4.7	
FMI 3336		1st dir.	31429	315	99	9.7	

remarks: CC139C = Hitco CC 139 C, K-Karb = Kaiser Aerotech K-Karb 1200, CF 322 = Schunk Kohlenstofftechnik CF 322, CX-20U = Toyo Tanso CX-20U, AMT and BMT = Mitsubishi Chem. Ind. AMT and BMT, FMI 3333 = FMI 3-3-3-3, FMI 3336 = FMI 3-3-3-6

srf. ground, 1400°C,3h: surface ground for removal of the surface layer, then baked to 1400°C for 3 hours

direction of beam incidence: (⊥): direction of beam incidence perpendicular to weave planes

(∥): direction of beam incidence parallel to weave planes

x shots on one sample: the same sample was exposed several times; the weight loss was measured after the last exposure

Table 2 (continued): List of samples tested, experimental parameters and weight losses of the samples during the experiments

material	cracking	erosion
2-d C-C (⊥)		
CC 139 C	no	4-5
KKarb 1200	no	5
CF 322	no	5
CX-20U	no	
AMT	no	4-5
BMT	no	4-5
2-d C-C (∥)		
CC 139 C	microcracks	2
KKarb 1200	cracks	3-4
CF 322	no	
CX-20U	microcracks	
4-d C-C		
FMI 3-3-3-3	cracks	2
FMI 3-3-3-6	cracks preexist.	2

Table 3: Summary of experimental results

Note: Cracks which occured in the experiments are stopped in the structure of the material. Fracture was not observed. The erosion behaviour is indicated by numbers 1 to 5, meaning: 1: very little erosion
2: little erosion
3: erosion similar to graphites
4: high erosion
5: very high erosion

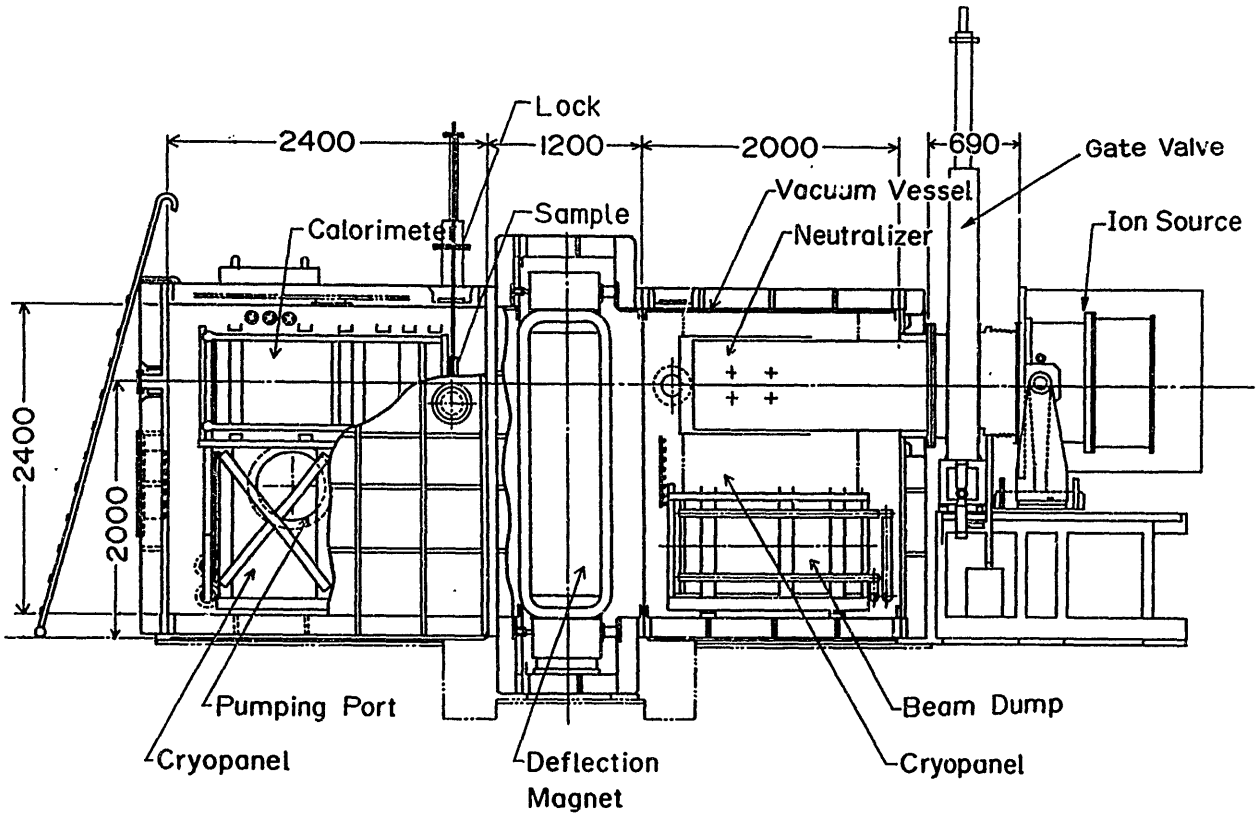

Figure 1: Schematic of the Neutral Beam Injection Test Stand used for materials tests on C-C composites

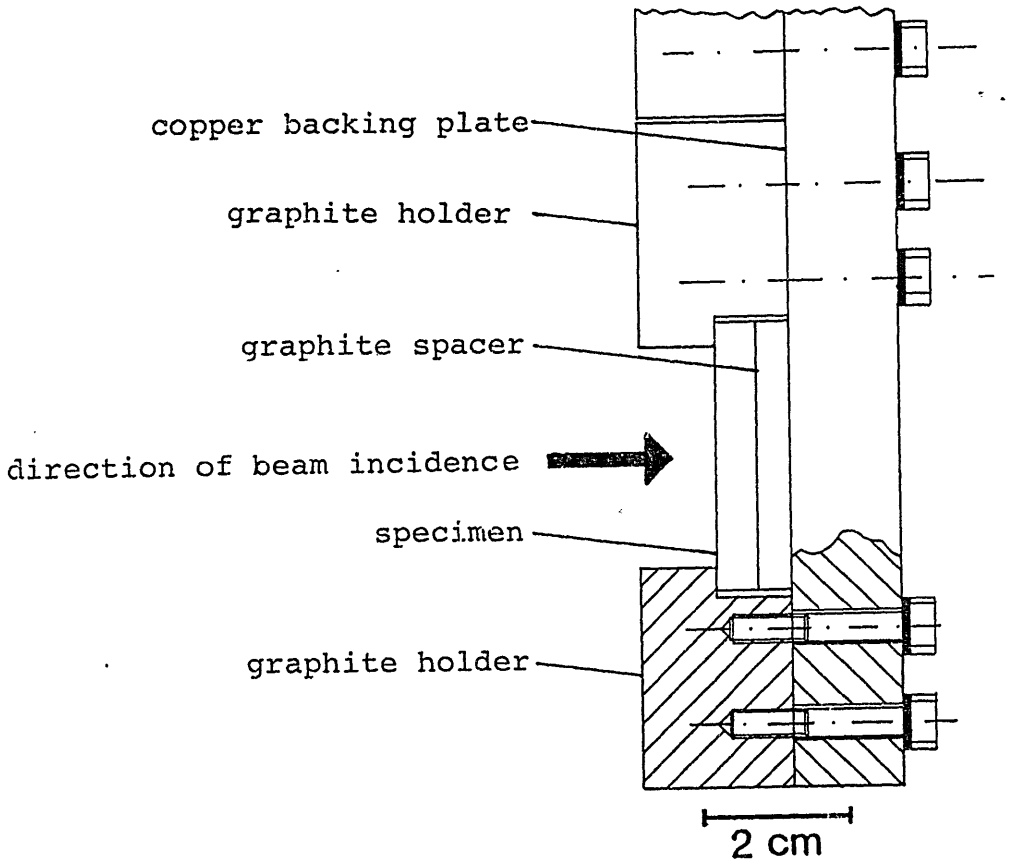

Figure 2: Attachment of C-C composite sample to the sample holder (copper backing plate)

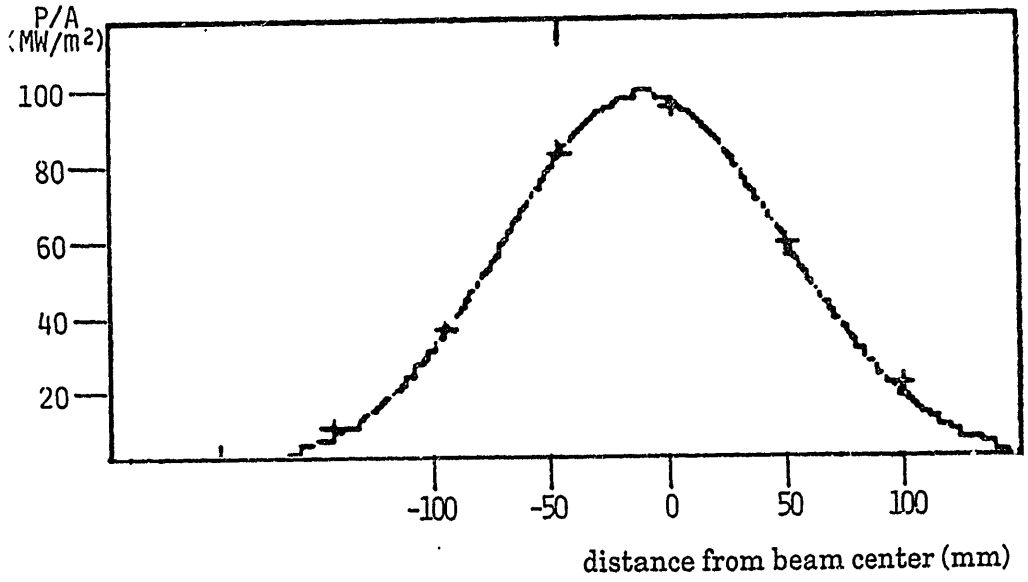

Figure 3: Power density distribution profile of the hydrogen beam

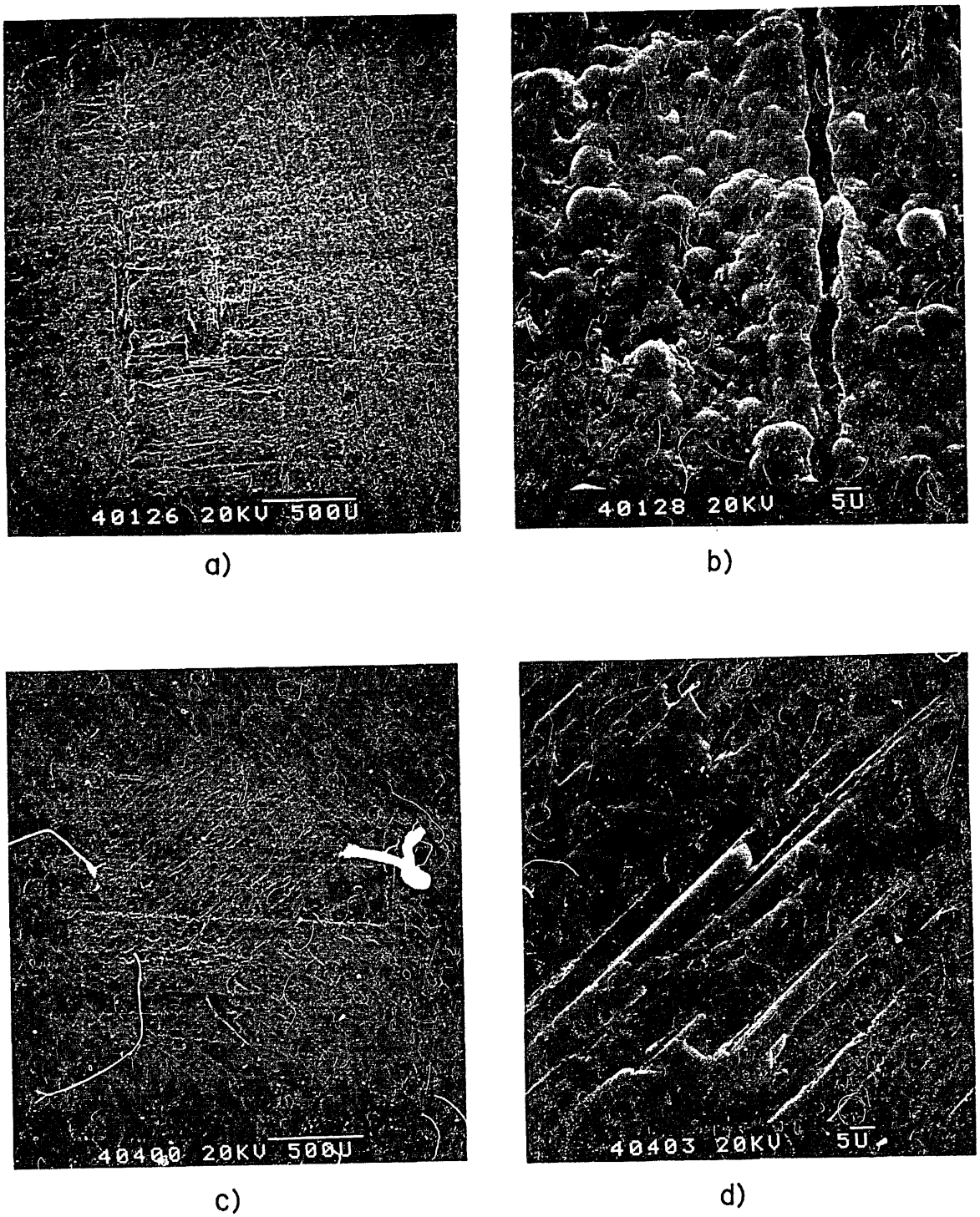

a) b)

c) d)

Figure 4: Hitco CC 139 C

a), b): surface in weave orientation, unirradiated

c), d): surface in weave orientation, coating removed by grinding, unirradiated

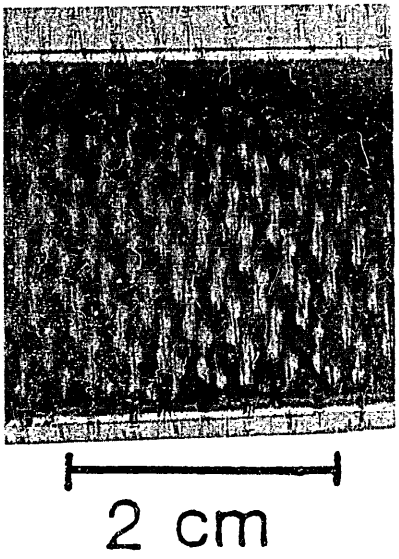

a) b)

Figure 5 a), b): Hitco CC 139 C
heat flux perpendicular to weave orientation (⊥),
pulse length 101 ms, power density 105 MW/m^2

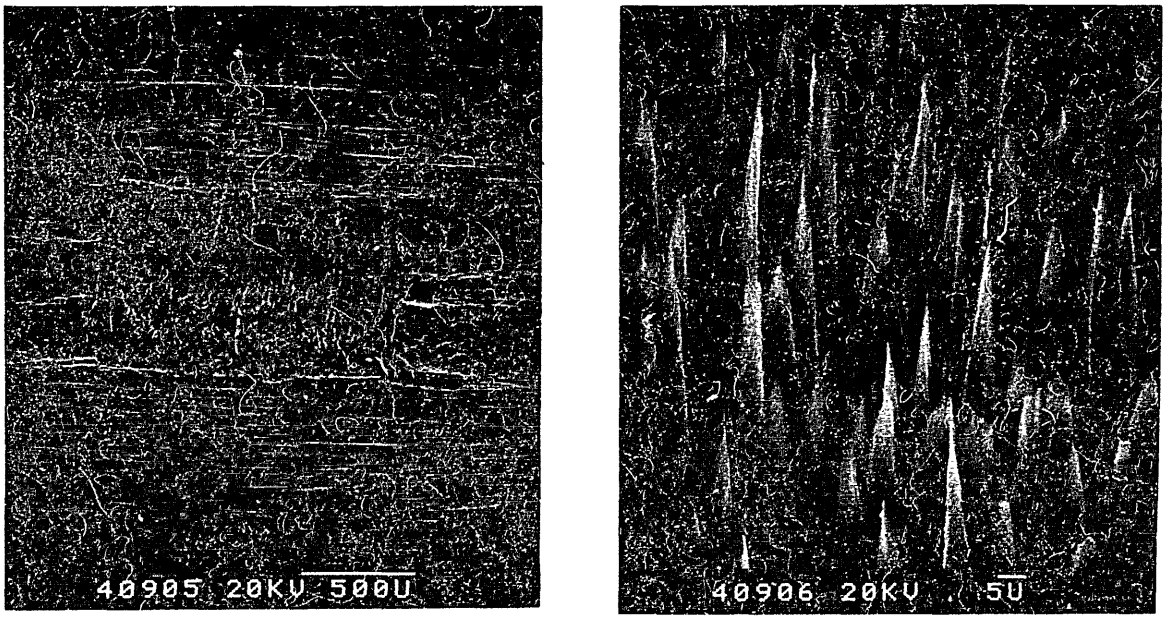

a) b)

Figure 6 a), b): Hitco CC 139 C
heat flux perpendicular to weave orientation (⊥),
5 pulses on the same sample

pulse length (ms)	power density (MW/m^2)
139	97
107	100
113	103
107	99
139	97

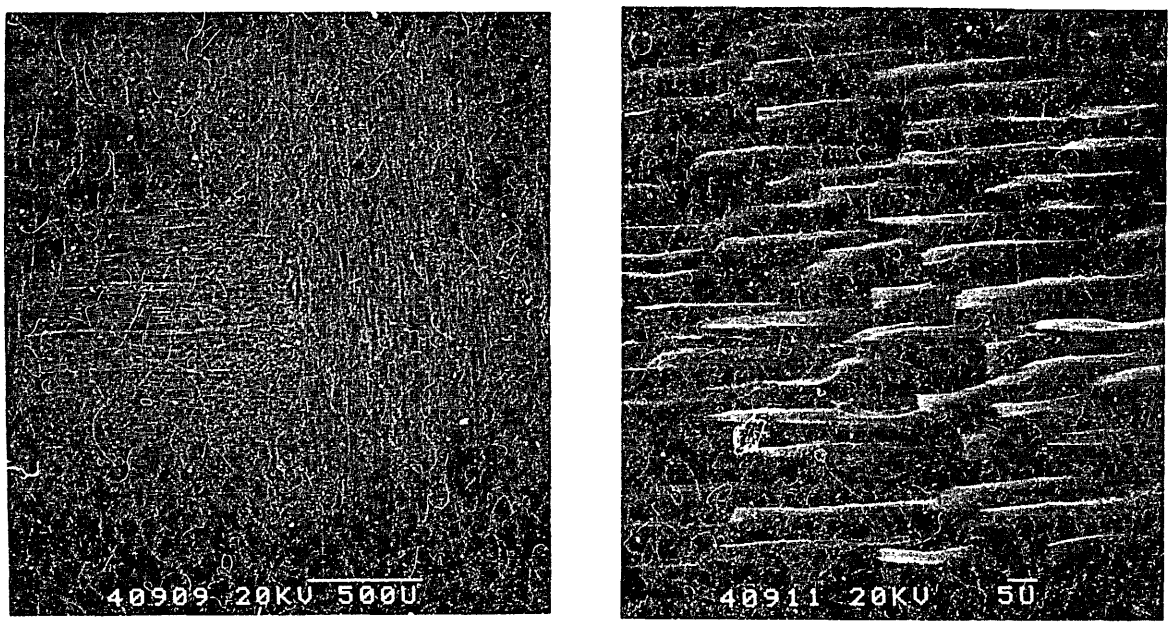

a) b)

Figure 7 a), b): Hitco CC 139 C, coating removed before irradiation, heat flux perpendicular to weave orientation (⊥), pulse length 145 ms, power density 97 MW/m^2

a)

b)

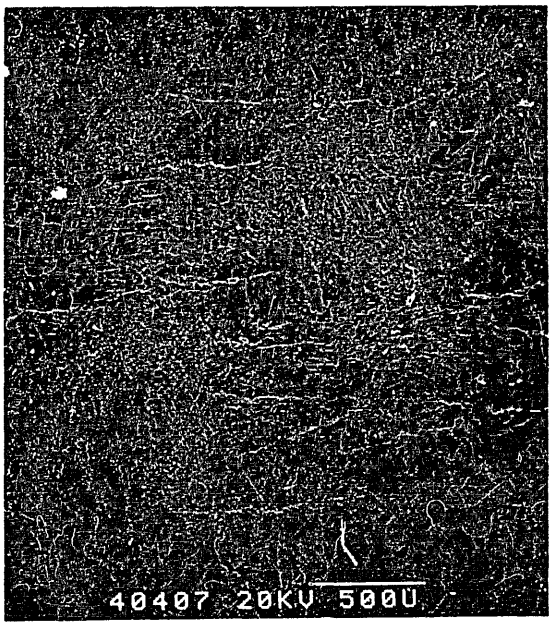

c)

d)

Figure 8: Kaiser Aerotech KKarb 1200
a), b): surface in weave orientation, unirradiated
c), d): surface in weave orientation, coating removed by grinding, unirradiated

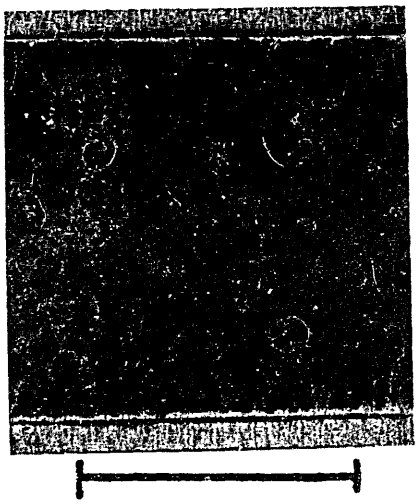

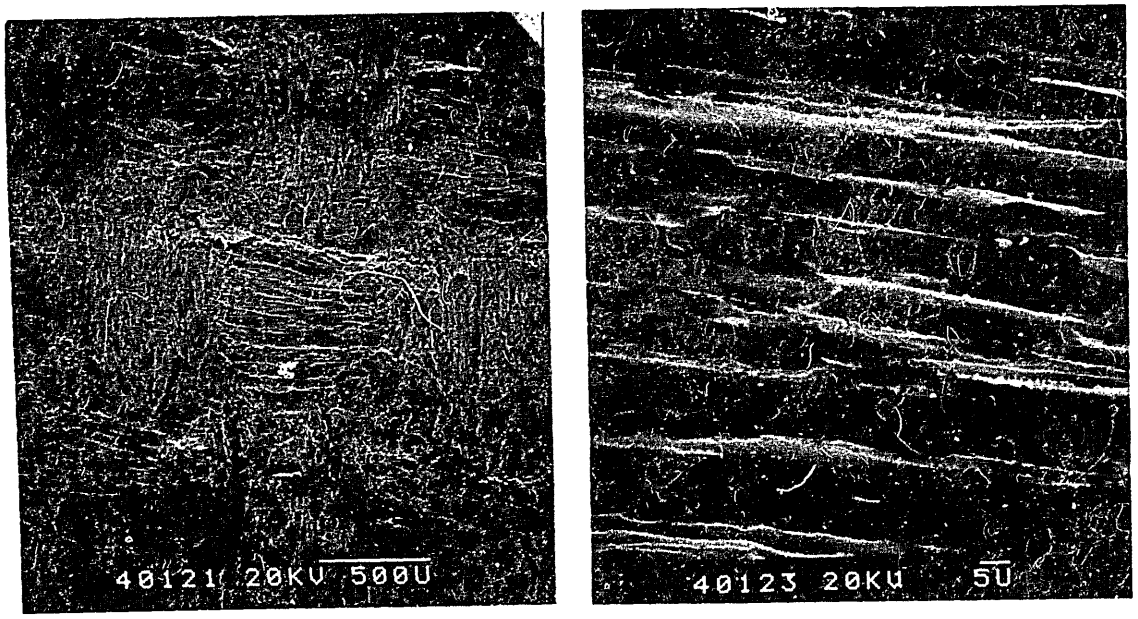

a) b)

Figure 9 a), b): Kaiser Aerotech KKarb 1200
heat flux perpendicular to weave orientation (⊥),
2 pulses on the same sample

pulse length (ms)	power density (MW/m^2)
69	110
76	105

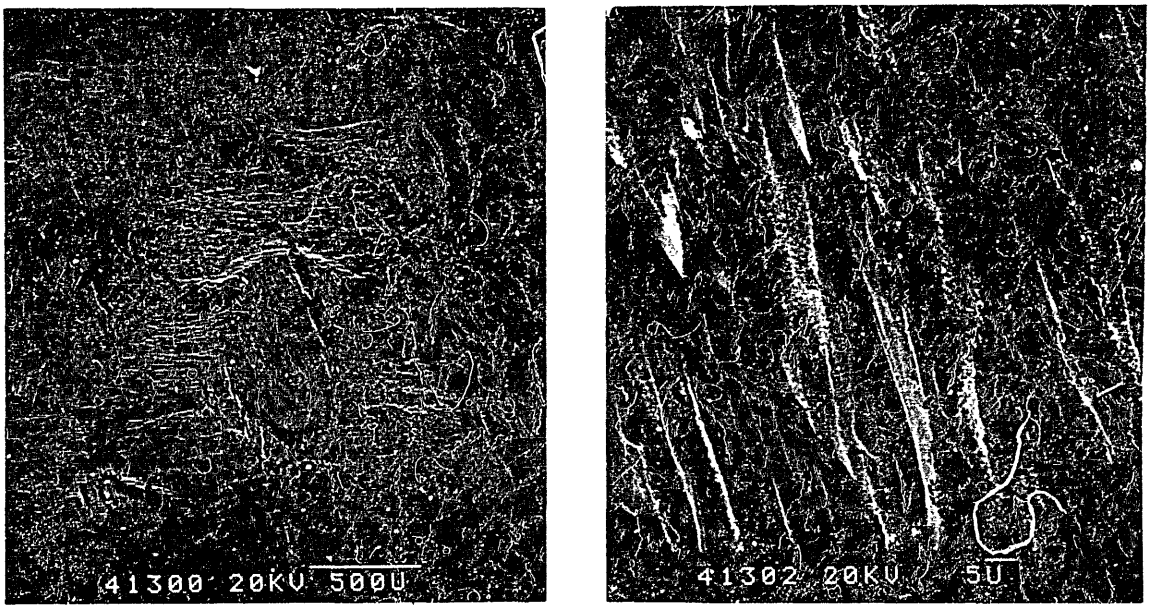

a) b)

Figure 10 a), b): Kaiser Aerotech KKarb 1200, coating removed before irradiation, heat flux perpendicular to weave orientation (⊥), pulse length 76 ms, power density 100 MW/m^2

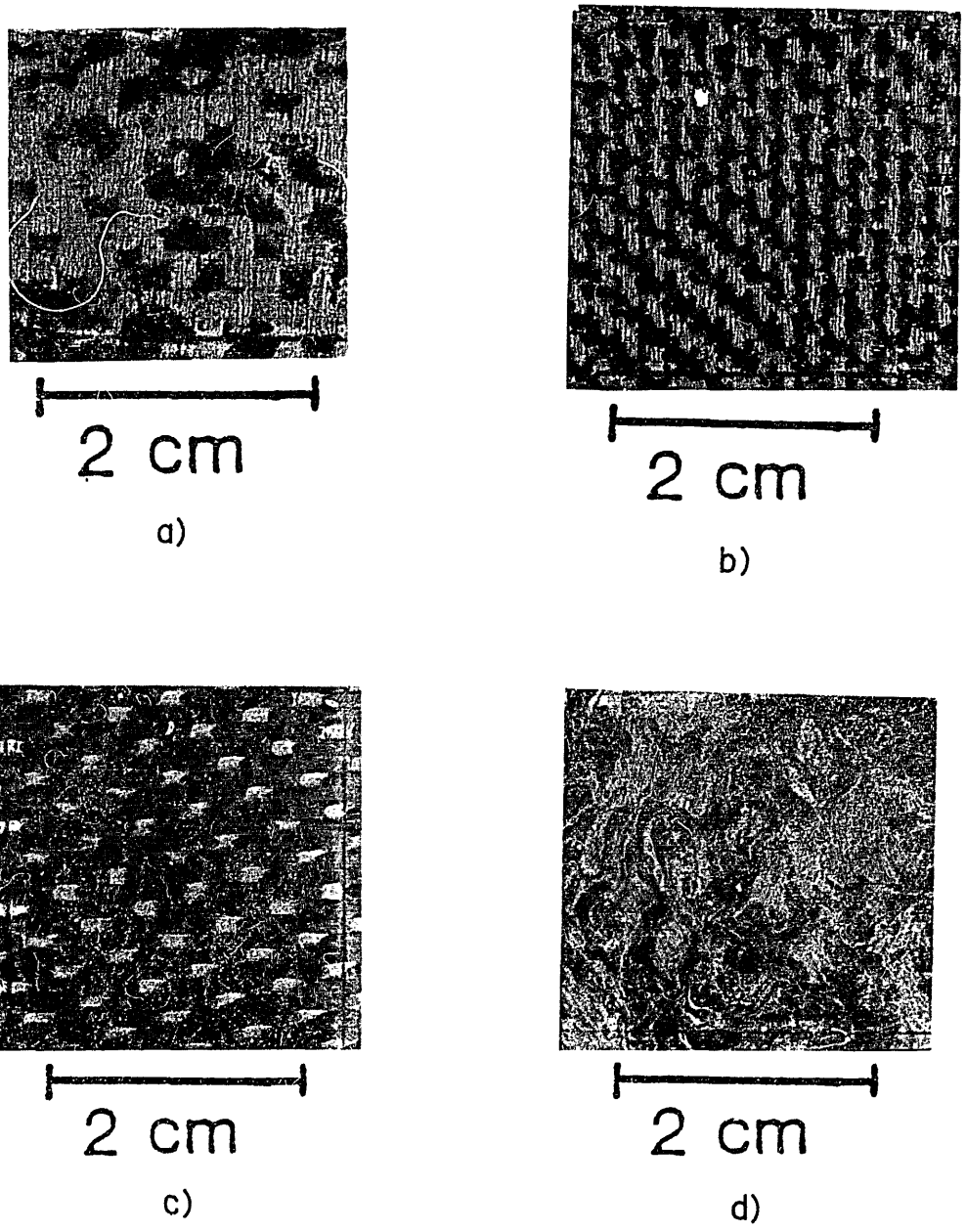

Figure 11 a): Schunk Kohlenstofftechnik CF 322
pulse length 69 ms, power density 102 MW/m^2
b): Toyo Tanso CX-20U
pulse length 76 ms, power density 101 MW/m^2
c): Mitsubishi Chemical Industries AMT
pulse length 107 ms, power density 99 MW/m^2
d): Mitsubishi Chemical Industries BMT
pulse length 120 ms, power density 103 MW/m^2

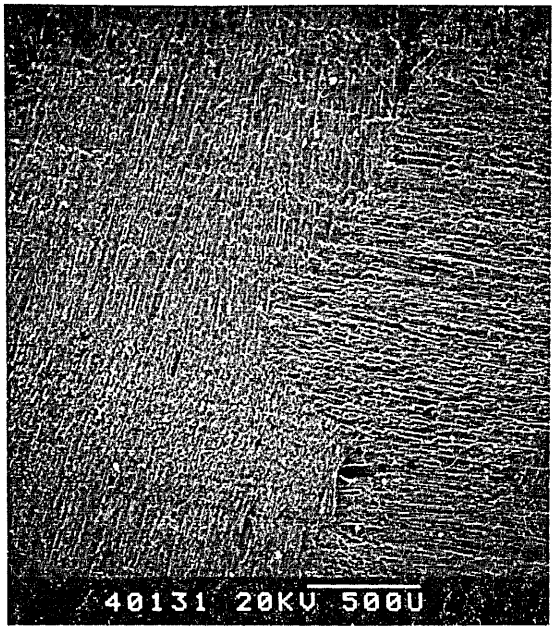

a)

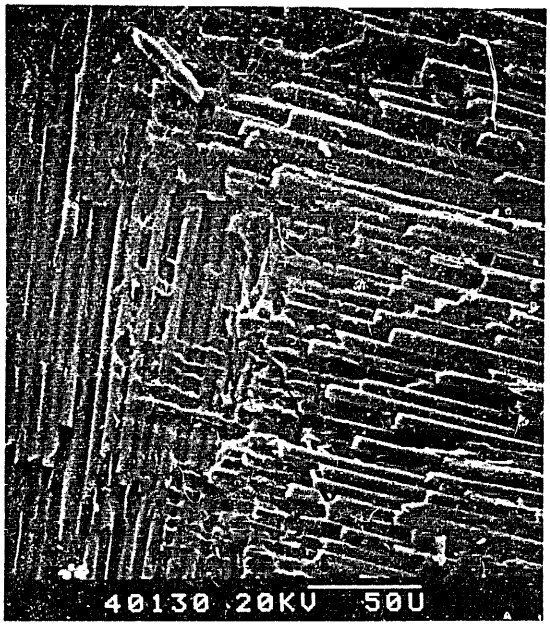

b)

c)

d)

Figure 12: Schunk Kohlenstofftechnik CF 322
a), b): surface in weave orientation, unirradiated
c), d): heat flux perpendicular to weave orientation (⊥),
pulse length 69 ms, power density 102 MW/m^2

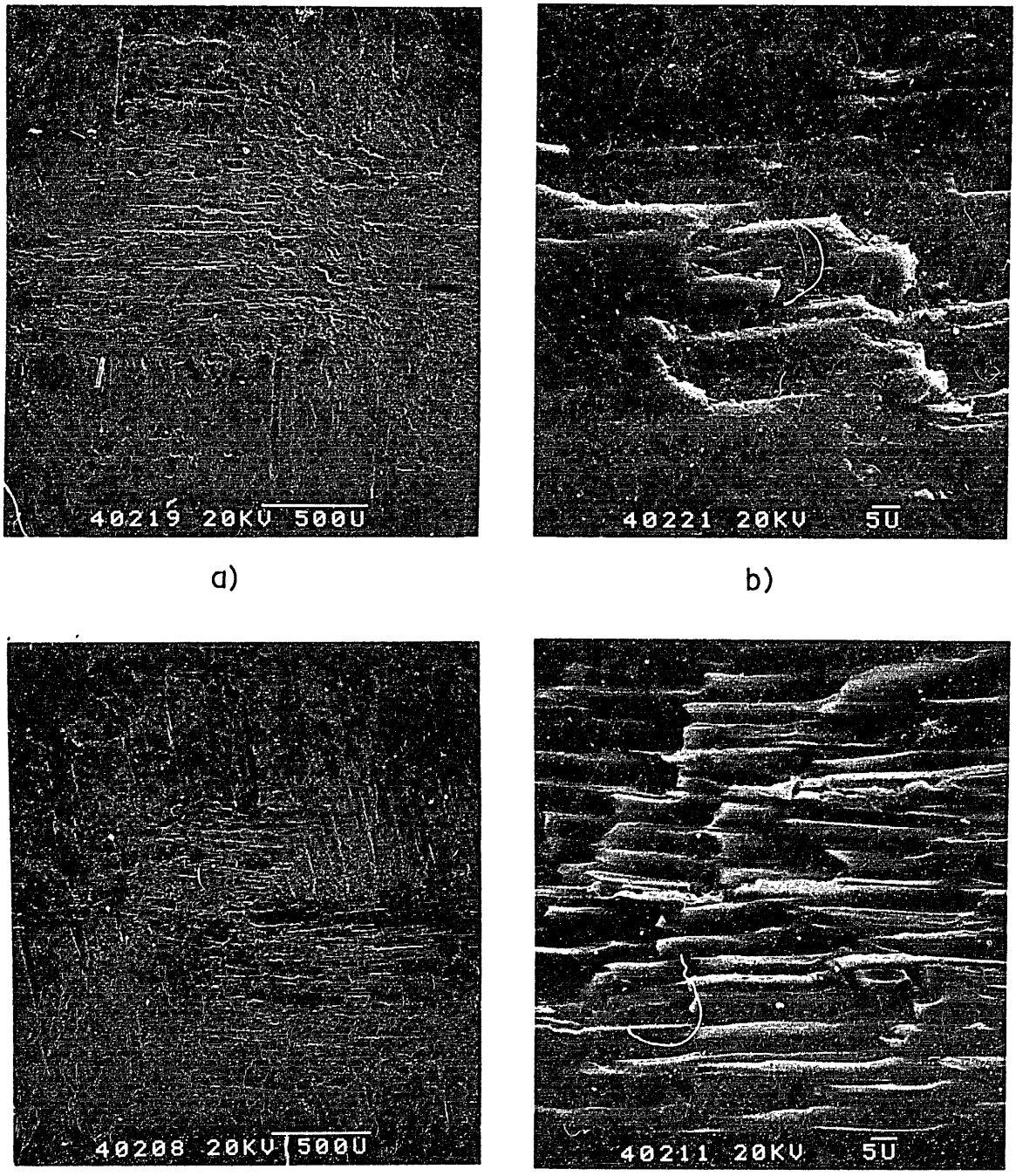

Figure 13: Toyo Tanso CX-20U
a), b): surface in weave orientation, unirradiated
c), d): heat flux perpendicular to weave orientation (⊥), pulse length 76 ms, power density 101 MW/m^2

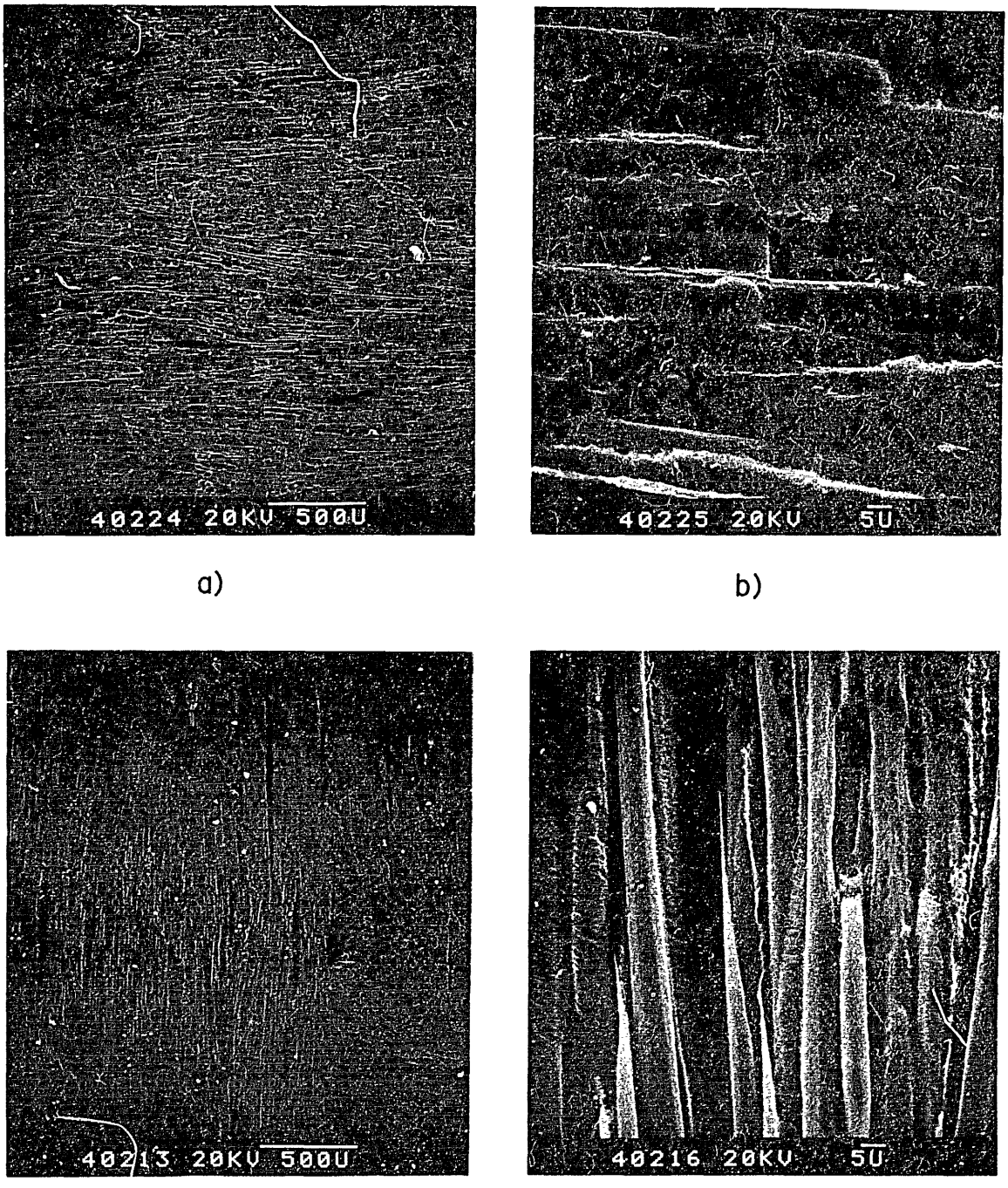

Figure 14: Mitsubishi Chemical Industries AMT
a), b): surface in weave orientation, unirradiated
c), d): heat flux perpendicular to weave orientation (⊥),
pulse length 107 ms, power density 99 MW/m^2

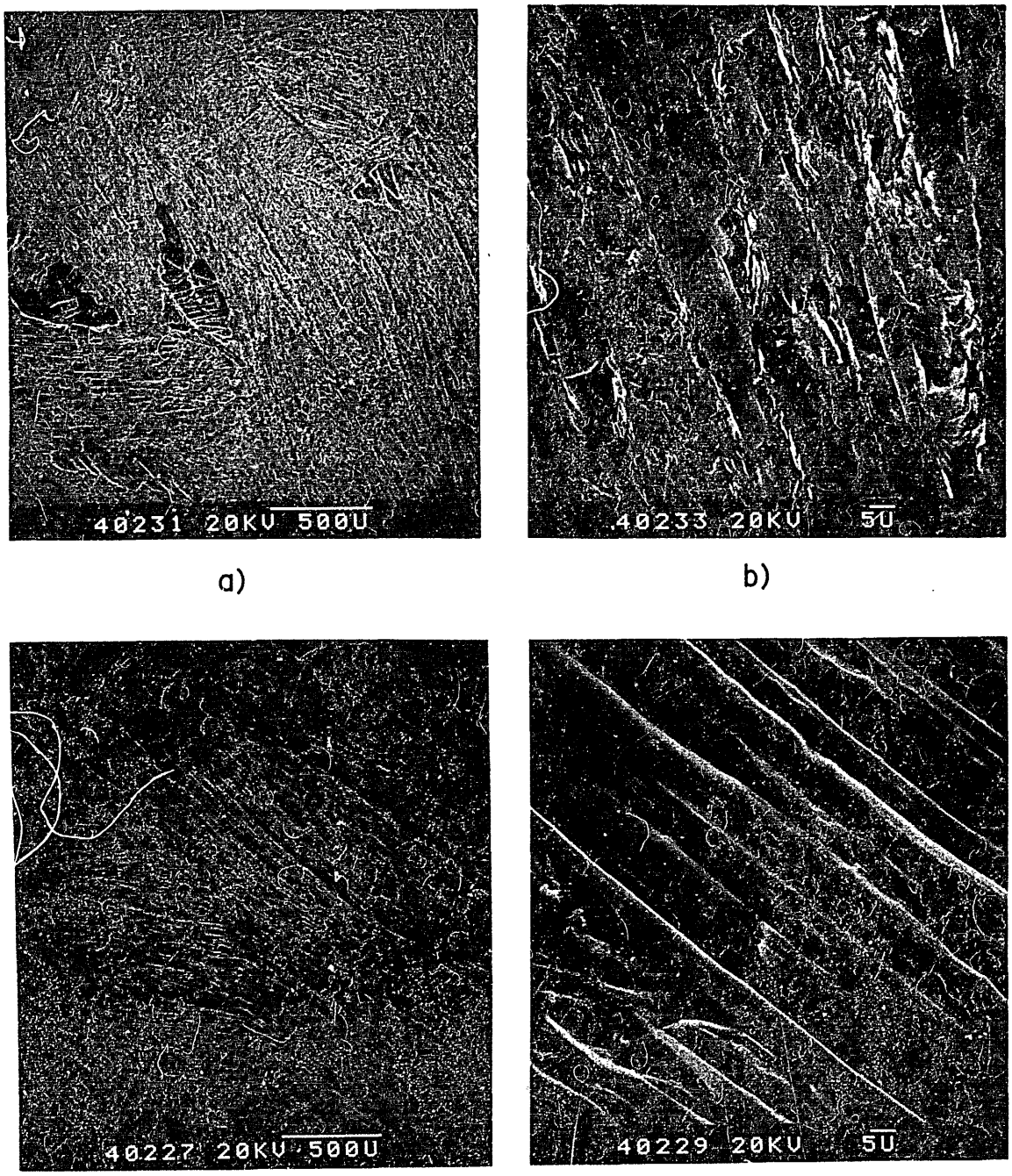

a) b)

c) d)

Figure 15: Mitsubishi Chemical Industries BMT
a), b): surface in weave orientation, unirradiated
c), d): heat flux perpendicular to weave orientation ($\perp$), pulse length 120 ms, power density 103 MW/m^2

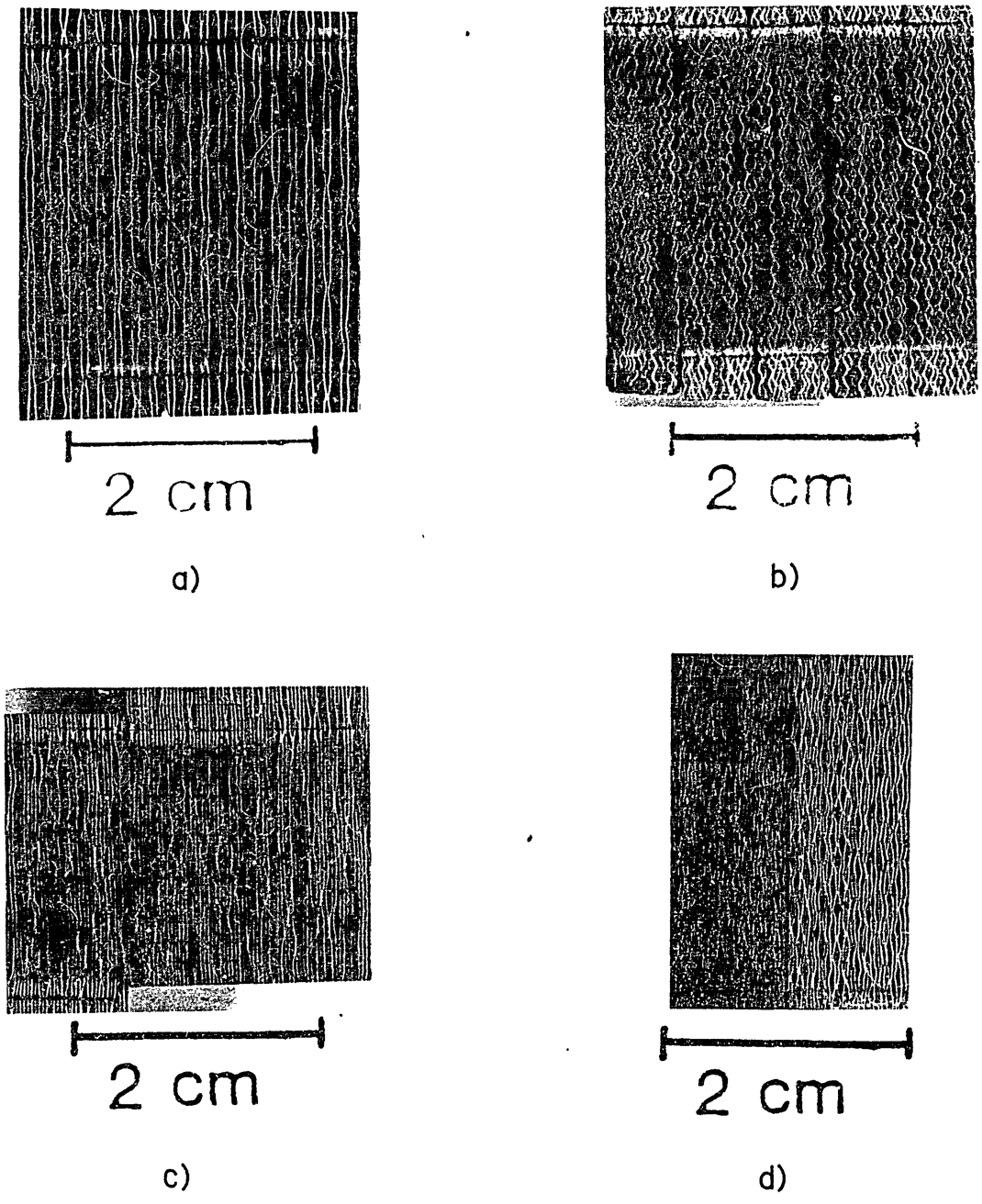

Figure 16: Irradiated surfaces cut against weave orientation

a): Hitco CC 139 C
pulse length 208 ms, power density 117 MW/m^2

b): Kaiser Aerotech KKarb 1200
pulse length 164 ms, power density 102 MW/m^2

c): Schunk Kohlenstofftechnik CF 322
pulse length 277 ms, power density 99 MW/m^2

d): Toyo Tanso CX-20U
pulse length 120 ms, power density 103 MW/m^2

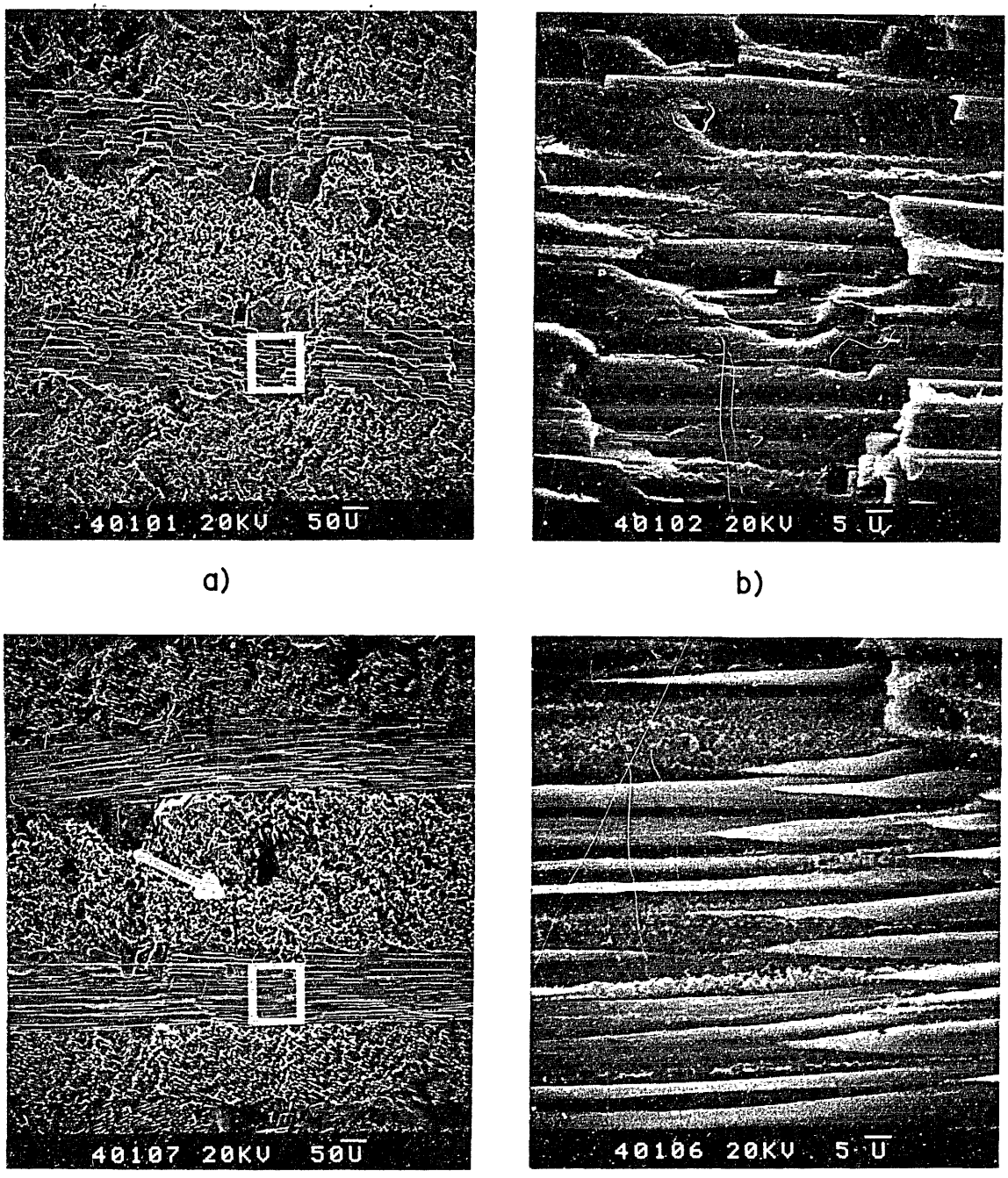

a) b)

c) d)

Figure 17: Hitco CC 139 C

a), b): Unirradiated surfaces cut against weave orientation

c), d): heat flux parallel to weave orientation (//), pulse length 208 ms, power density 117 MW/m^2

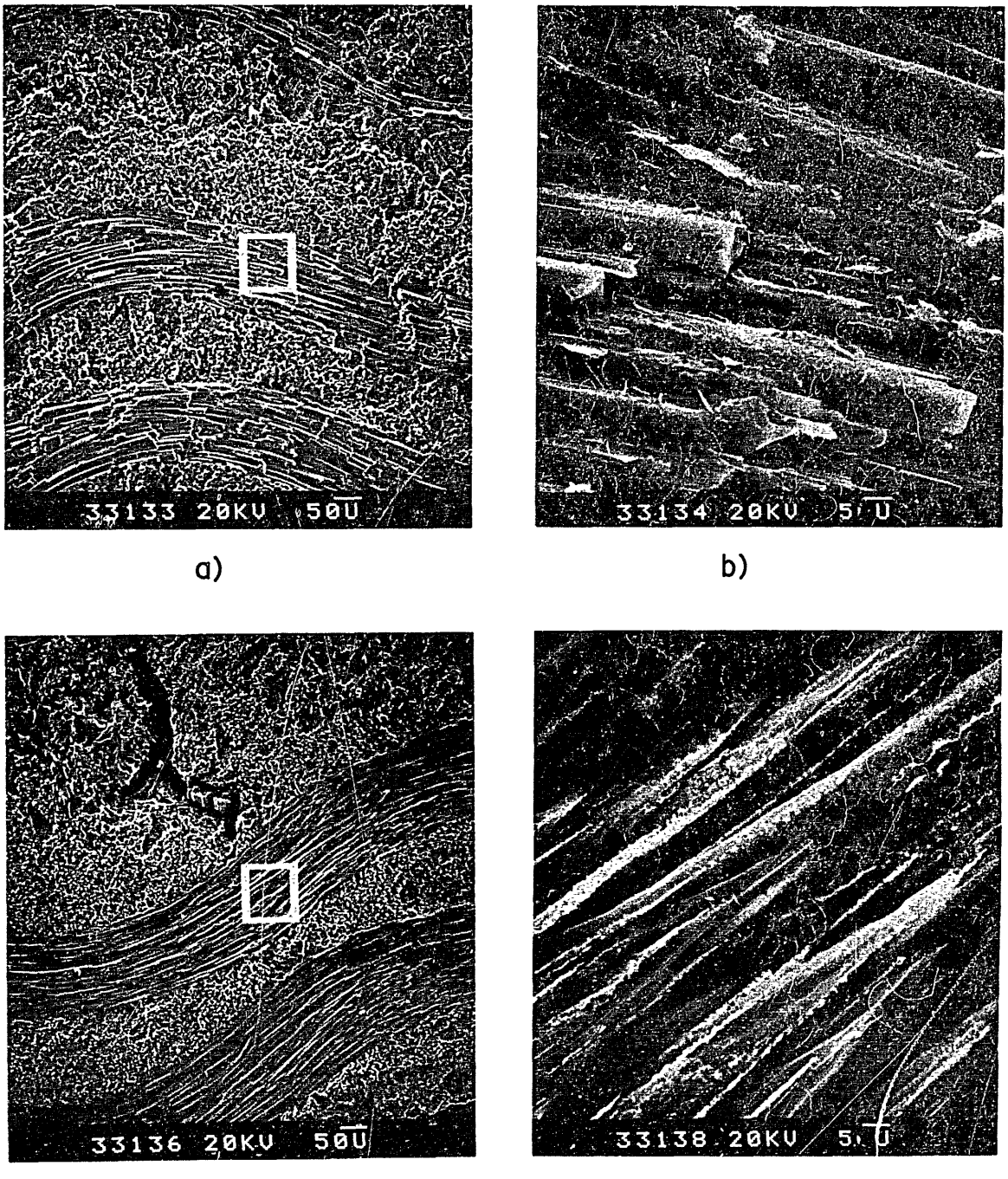

Figure 18: Kaiser Aerotech KKarb 1200
a), b): Unirradiated surfaces cut against weave orientation
c), d): heat flux parallel to weave orientation (//),
pulse length 164 ms, power density 102 MW/m^2

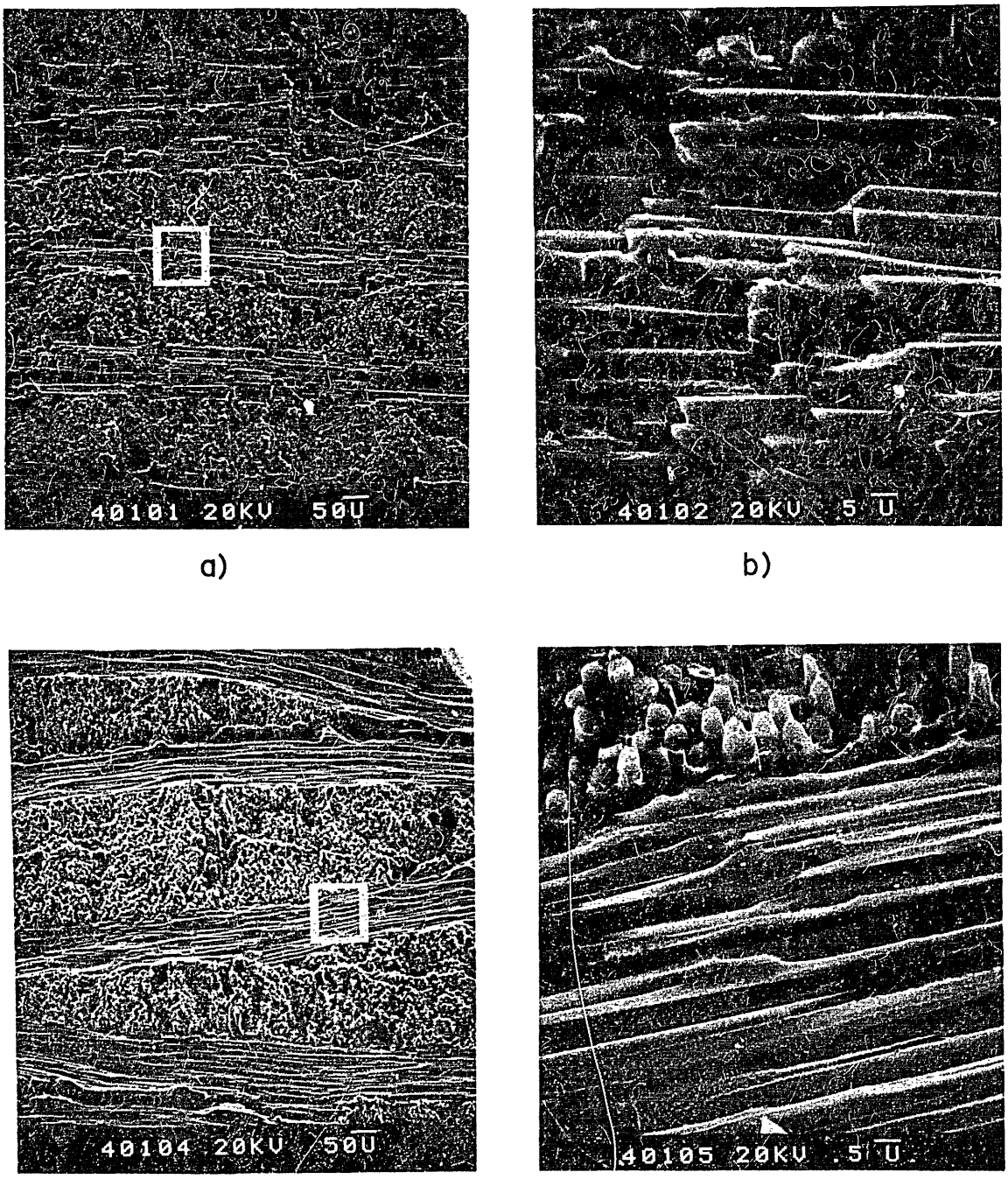

Figure 19: Schunk Kohlenstofftechnik CF 322
a), b): Unirradiated surfaces cut against weave orientation
c), d): heat flux parallel to weave orientation (//),
pulse length 277 ms, power density 99 MW/m^2

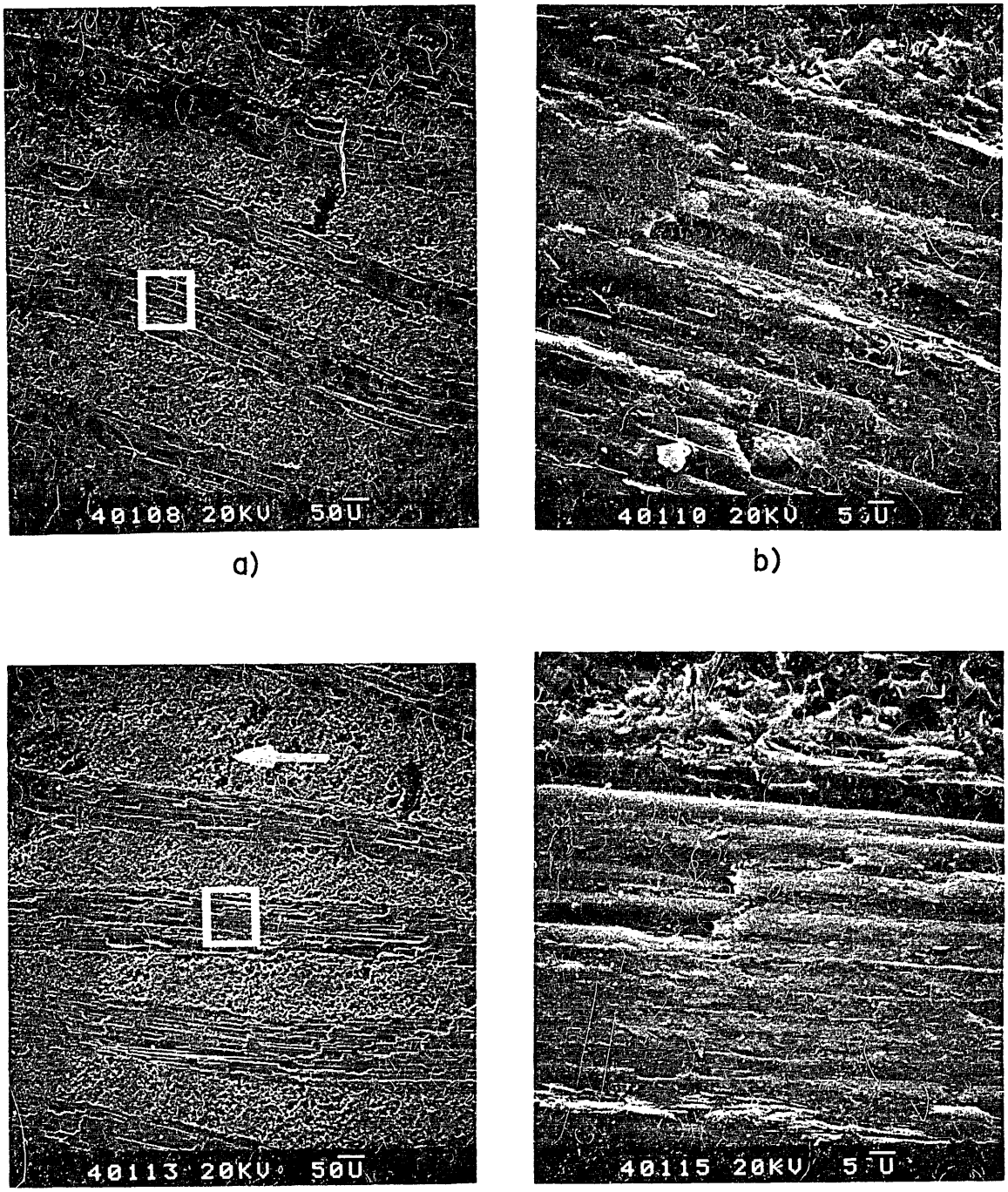

Figure 20: Toyo Tanso CX-20U

a), b): Unirradiated surfaces cut against weave orientation

c), d): heat flux parallel to weave orientation (||),
pulse length 170 ms, power density 96 MW/m^2

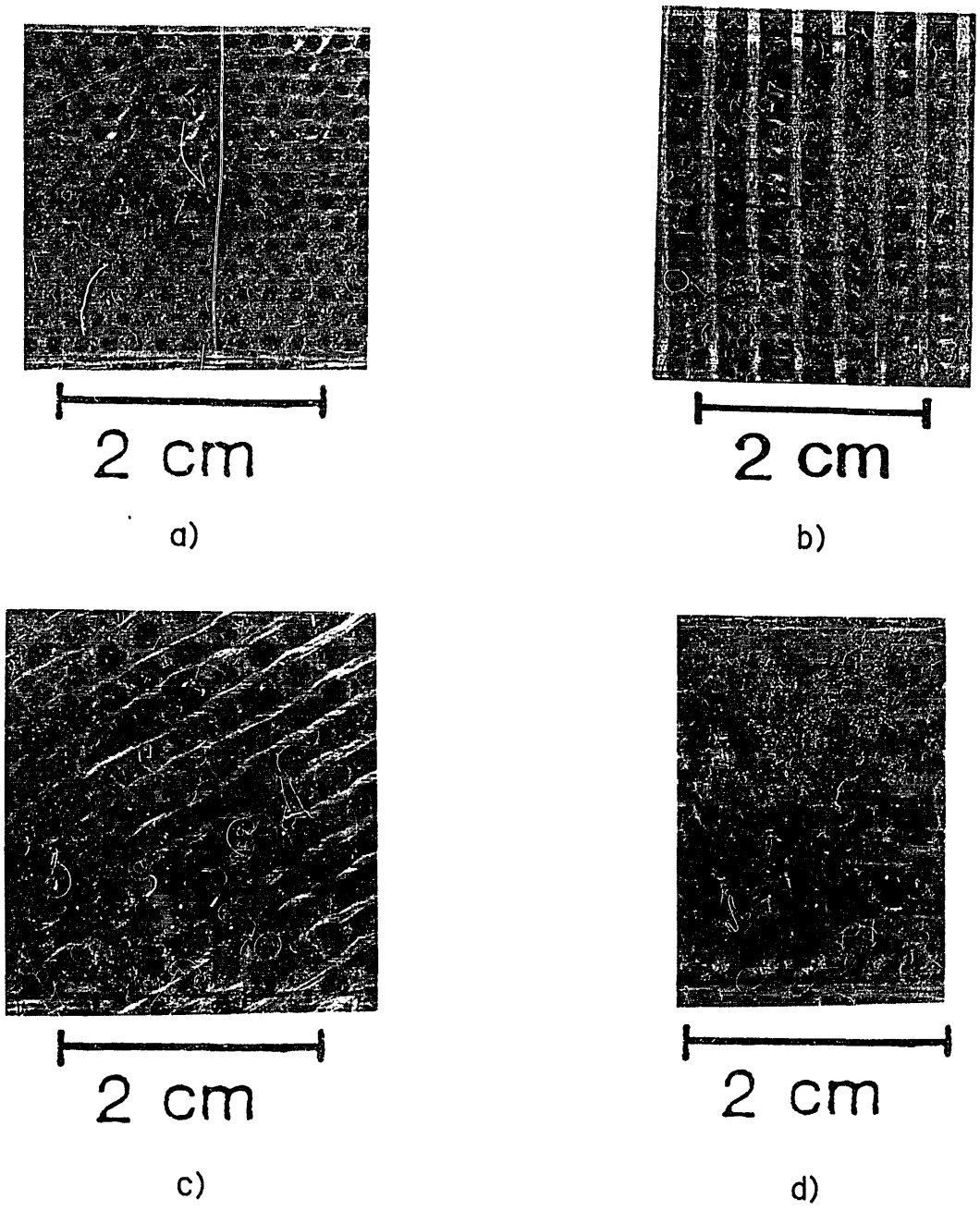

Figure 21 a): FMI 3-3-3-3, 1st direction
pulse length 258 ms, power density 102 MW/m^2
b): FMI 3-3-3-3, 2nd direction
pulse length 202 ms, power density 102 MW/m^2
c): FMI 3-3-3-6, 1st direction
pulse length 315 ms, power density 108 MW/m^2
d): FMI 3-3-3-6, 2nd direction
pulse length 315 ms, power density 99 MW/m^2

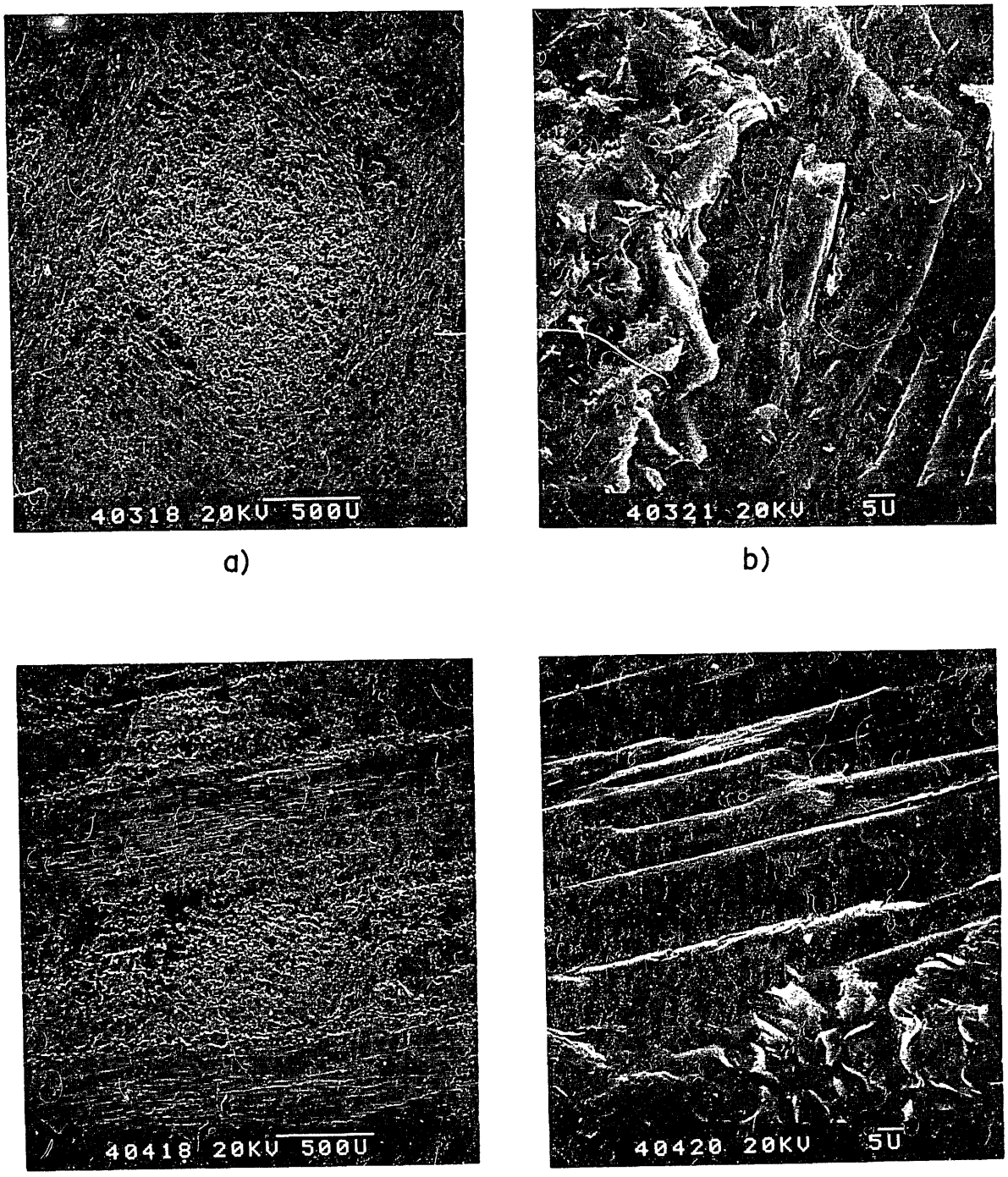

a) b)

c) d)

Figure 22: FMI 3-3-3-3, 1st direction
a), b): unirradiated
c), d): pulse length 258 ms, power density 102 MW/m^2

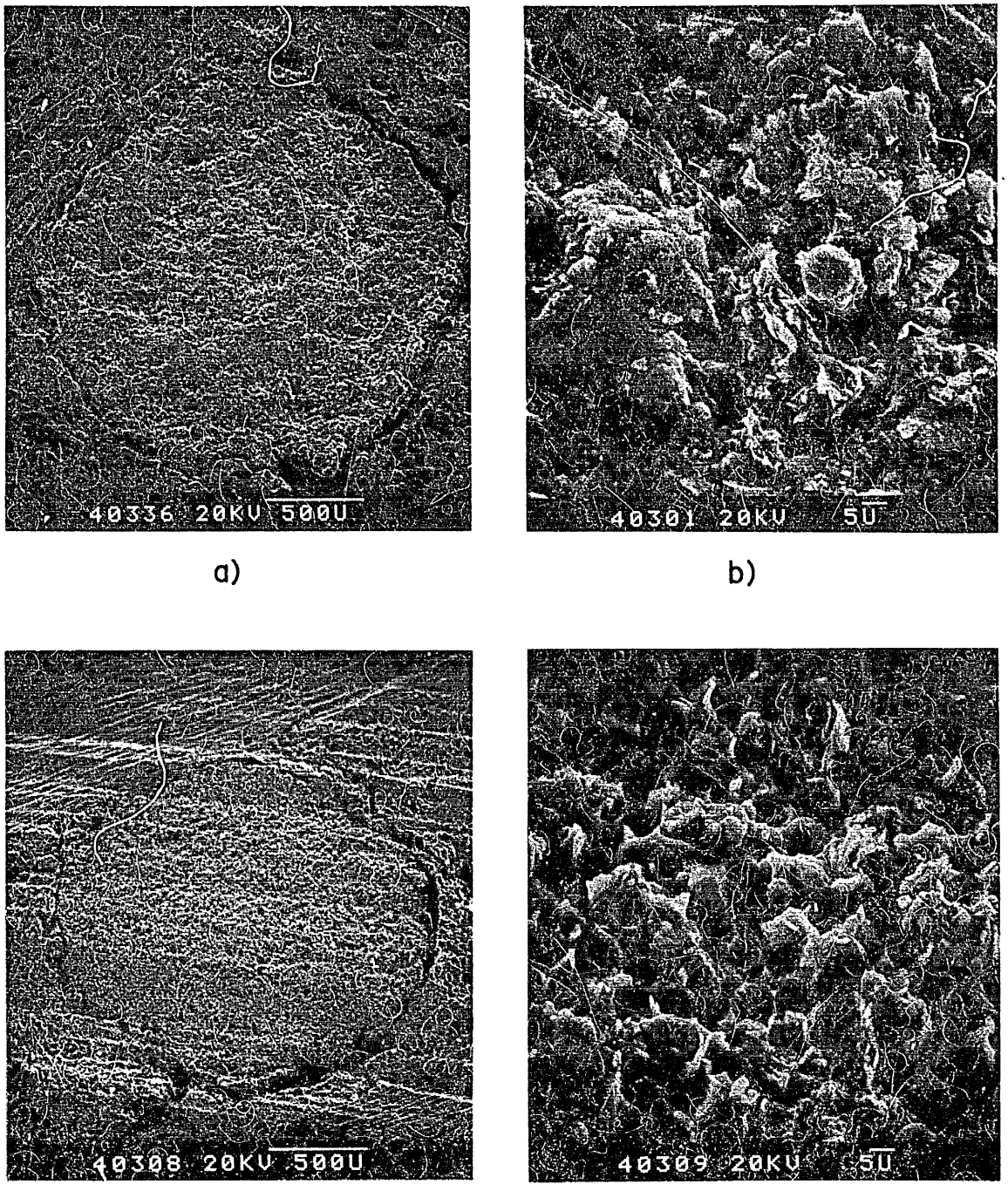

Figure 23: FMI 3-3-3-6, 1st direction
a), b): unirradiated
c), d): pulse length 315 ms, power density 108 MW/m^2

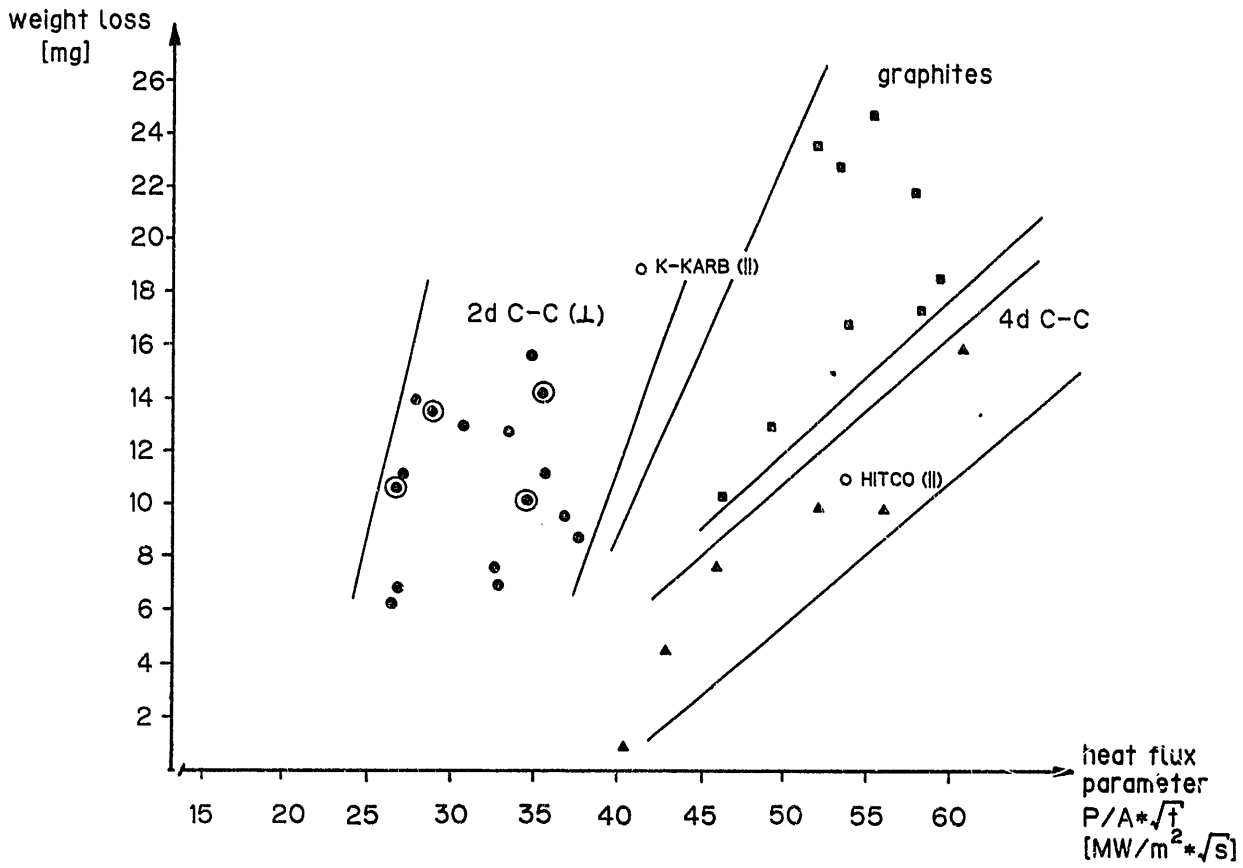

Figure 24: Erosion of carbon materials as function of the incident heat flux, indicated by the heat flux parameter F. Clearly the different erosion behaviour of 2-d C-C composites, graphites, and 4-d C-C composites can be distinguished (cf. 5.1).

Note: -Encircled points are mean values of samples subjected to multiple shots.

-The results obtained with the 2-d composite CF 322 have been corrected by 44% due to the different size of these samples.

LIST OF IPPJ-AM REPORTS

IPPJ-AM-1* "Cross Sections for Charge Transfer of Hydrogen Beams in Gases and Vapors in the Energy Range 10 eV–10 keV"
H. Tawara (1977) [Published in Atomic Data and Nuclear Data Tables 22, 491 (1978)]

IPPJ-AM-2* "Ionization and Excitation of Ions by Electron Impact –Review of Empirical Formulae–"
T. Kato (1977)

IPPJ-AM-3 "Grotrian Diagrams of Highly Ionized Iron FeVIII-FeXXVI"
K. Mori, M. Otsuka and T. Kato (1977) [Published in Atomic Data and Nuclear Data Tables 23, 196 (1979)]

IPPJ-AM-4 "Atomic Processes in Hot Plasmas and X-Ray Emission"
T. Kato (1978)

IPPJ-AM-5* "Charge Transfer between a Proton and a Heavy Metal Atom"
S. Hiraide, Y. Kigoshi and M. Matsuzawa (1978)

IPPJ-AM-6* "Free-Free Transition in a Plasma –Review of Cross Sections and Spectra–"
T. Kato and H. Narumi (1978)

IPPJ-AM-7* "Bibliography on Electron Collisions with Atomic Positive Ions: 1940 Through 1977"
K. Takayanagi and T. Iwai (1978)

IPPJ-AM-8 "Semi-Empirical Cross Sections and Rate Coefficients for Excitation and Ionization by Electron Collision and Photoionization of Helium"
T. Fujimoto (1978)

IPPJ-AM-9 "Charge Changing Cross Sections for Heavy-Particle Collisions in the Energy Range from 0.1 eV to 10 MeV I. Incidence of He, Li, Be, B and Their Ions"
Kazuhiko Okuno (1978)

IPPJ-AM-10 "Charge Changing Cross Sections for Heavy-Particle Collisions in the Energy Range from 0.1 eV to 10 MeV II. Incidence of C, N, O and Their Ions"
Kazuhiko Okuno (1978)

IPPJ-AM-11 "Charge Changing Cross Sections for Heavy-Particle Collisions in the Energy Range from 0.1 eV to 10 MeV III. Incidence of F, Ne, Na and Their Ions"
Kazuhiko Okuno (1978)

IPPJ-AM-12* "Electron Impact Excitation of Positive Ions Calculated in the Coulomb-Born Approximation –A Data List and Comparative Survey–"
S. Nakazaki and T. Hashino (1979)

IPPJ-AM-13 "Atomic Processes in Fusion Plasmas – Proceedings of the Nagoya Seminar on Atomic Processes in Fusion Plasmas Sept. 5-7, 1979"
Ed. by Y. Itikawa and T. Kato (1979)

IPPJ-AM-14 "Energy Dependence of Sputtering Yields of Monatomic Solids"
N. Matsunami, Y. Yamamura, Y. Itikawa, N. Itoh, Y. Kazumata, S. Miyagawa, K. Morita and R. Shimizu (1980)

IPPJ-AM-15 "Cross Sections for Charge Transfer Collisions Involving Hydrogen Atoms"
Y. Kaneko, T. Arikawa, Y. Itikawa, T. Iwai, T. Kato, M. Matsuzawa, Y. Nakai, K. Okubo, H. Ryufuku, H. Tawara and T. Watanabe (1980)

IPPJ-AM-16 "Two-Centre Coulomb Phaseshifts and Radial Functions"
H. Nakamura and H. Takagi (1980)

IPPJ-AM-17 "Empirical Formulas for Ionization Cross Section of Atomic Ions for Electron Collisions –Critical Review with Compilation of Experimental Data–"
Y. Itikawa and T. Kato (1981)

IPPJ-AM-18 "Data on the Backscattering Coefficients of Light Ions from Solids"
T. Tabata, R. Ito, Y. Itikawa, N. Itoh and K. Morita (1981) [Published in Atomic Data and Nuclear Data Tables 28, 493 (1983)]

IPPJ-AM-19 "Recommended Values of Transport Cross Sections for Elastic Collision and Total Collision Cross Section for Electrons in Atomic and Molecular Gases"
M. Hayashi (1981)

IPPJ-AM-20 "Electron Capture and Loss Cross Sections for Collisions between Heavy Ions and Hydrogen Molecules"
Y. Kaneko, Y. Itikawa, T. Iwai, T. Kato, Y. Nakai, K. Okuno and H. Tawara (1981)

IPPJ-AM-21 "Surface Data for Fusion Devices – Proceedings of the U.S–Japan Workshop on Surface Data Review Dec. 14-18, 1981"
Ed. by N. Itoh and E.W. Thomas (1982)

IPPJ-AM-22 "Desorption and Related Phenomena Relevant to Fusion Devices"
Ed. by A. Koma (1982)

IPPJ-AM-23 "Dielectronic Recombination of Hydrogenic Ions"
T. Fujimoto, T. Kato and Y. Nakamura (1982)

IPPJ-AM-24 "Bibliography on Electron Collisions with Atomic Positive Ions: 1978 Through 1982 (Supplement to IPPJ-AM-7)"
Y. Itikawa (1982) [Published in Atomic Data and Nuclear Data Tables 31, 215 (1984)]

IPPJ-AM-25 "Bibliography on Ionization and Charge Transfer Processes in Ion-Ion Collision"
H. Tawara (1983)

IPPJ-AM-26 "Angular Dependence of Sputtering Yields of Monatomic Solids"
Y. Yamamura, Y. Itikawa and N. Itoh (1983)

IPPJ-AM-27 "Recommended Data on Excitation of Carbon and Oxygen Ions by Electron Collisions"
Y. Itikawa, S. Hara, T. Kato, S. Nakazaki, M.S. Pindzola and D.H. Crandall (1983) [Published in Atomic Data and Nuclear Data Tables 33, 149 (1985)]

IPPJ-AM-28 "Electron Capture and Loss Cross Sections for Collisions Between Heavy Ions and Hydrogen Molecules (Up-dated version of IPPJ-AM-20)
H. Tawara, T. Kato and Y. Nakai (1983) [Published in Atomic Data and Nuclear Data Tables 32, 235 (1985)]

IPPJ-AM-29 "Bibliography on Atomic Processes in Hot Dense Plasmas"
T. Kato, J. Hama, T. Kagawa, S. Karashima, N. Miyanaga, H. Tawara, N. Yamaguchi, K. Yamamoto and K. Yonei (1983)

IPPJ-AM-30 "Cross Sections for Charge Transfers of Highly Ionized Ions in Hydrogen Atoms (Up-dated version of IPPJ-AM-15)"
H. Tawara, T. Kato and Y. Nakai (1983) [Published in Atomic Data and Nuclear Data Tables 32, 235 (1985)]

IPPJ-AM-31 "Atomic Processes in Hot Dense Plasmas"
T. Kagawa, T. Kato, T. Watanabe and S. Karashima (1983)

IPPJ-AM-32 "Energy Dependence of the Yields of Ion-Induced Sputtering of Monatomic Solids"
N. Matsunami, Y. Yamamura, Y. Itikawa, N. Itoh, Y. Kazumata, S. Miyagawa, K. Morita, R. Shimizu and H. Tawara (1983) [Published in Atomic Data and Nuclear Data Tables 31, 1 (1984)]

IPPJ-AM-33 "Proceedings on Symposium on Atomic Collision Data for Diagnostics and Modelling of Fusion Plasmas, Aug. 29 – 30, 1983"
Ed. by H. Tawara (1983)

IPPJ-AM-34 "Dependence of the Backscattering Coefficients of Light Ions upon Angle of Incidence"
T. Tabata, R. Ito, Y. Itikawa, N. Itoh, K. Morita and H. Tawara (1984)

IPPJ-AM-35 "Proceedings of Workshop on Synergistic Effects in Surface Phenomena Related to Plasma-Wall Interactions, May 21 – 23, 1984"
Ed. by N. Itoh, K. Kamada and H. Tawara (1984) [Published in Radiation Effects 89, 1 (1985)]

IPPJ-AM-36 "Equilibrium Charge State Distributions of Ions ($Z_1 \geqq 4$) after Passage through Foils – Compilation of Data after 1972"
K. Shima, T. Mikumo and H. Tawara (1985) [Published in Atomic Data and Nuclear Data Tables 34, 357 (1986)]

IPPJ-AM-37 "Ionization Cross Sections of Atoms and Ions by Electron Impact"
H. Tawara, T. Kato and M. Ohnishi (1985)

IPPJ-AM-38 "Rate Coefficients for the Electron-Impact Excitations of C-like Ions"
Y. Itikawa (1985)

IPPJ-AM-39 "Proceedings of the Japan-U.S. Workshop on Impurity and Particle Control, Theory and Modeling, Mar. 12 – 16, 1984"
Ed. by T. Kawamura (1985)

IPPJ-AM-40 "Low-Energy Sputterings with the Monte Carlo Program ACAT"
Y. Yamamura and Y. Mizuno (1985)

IPPJ-AM-41 "Data on the Backscattering Coefficients of Light Ions from Solids (a Revision)"
R. Ito, T. Tabata, N. Itoh, K. Morita, T. Kato and H. Tawara (1985)

IPPJ-AM-42 "Stopping Power Theories for Charged Particles in Inertial Confinement Fusion Plasmas (Emphasis on Hot and Dense Matters)"
S. Karashima, T. Watanabe, T. Kato and H. Tawara (1985)

IPPJ-AM-43 "The Collected Papers of Nice Project/IPP, Nagoya"
Ed. by H. Tawara (1985)

IPPJ-AM-44 "Tokamak Plasma Modelling and Atomic Processes"
Ed. by T. Kawamura (1986)

IPPJ-AM-45 Bibliography of Electron Transfer in Ion-Atom Collisions
H. Tawara, N. Shimakura, N. Toshima and T. Watanabe (1986)

IPPJ-AM-46 "Atomic Data Involving Hydrogens Relevant to Edge Plasmas"
H. Tawara, Y. Itikawa, Y. Itoh, T. Kato, H. Nishimura, S. Ohtani, H. Takagi, K. Takayanagi and M. Yoshino (1986)

IPPJ-AM-47 "Resonance Effects in Electron-Ion Collisions"
Ed. by H. Tawara and G. H. Dunn (1986)

IPPJ-AM-48 "Dynamic Processes of Highly Charged Ions (Proceedings)"
Ed. by Y. Kanai and S. Ohtani (1986)

IPPJ-AM-49 "Wavelengths of K X-Rays of Iron Ions"
T. Kato, S. Morita and H. Tawara (1987)

IPPJ-AM-50 "Proceedings of the Japan-U.S. Workshop P-92 on Plasma Material Interaction/High Heat Flux Data Needs for the Next Step Ignition and Steady State Devices, Jan. 26 – 30, 1987"
Ed. by A. Miyahara and K. L. Wilson (1987)

IPPJ-AM-51 "High Heat Flux Experiments on C-C Composite Materials by Hydrogen Beam at the 10MW Neutral Beam Injection Test Stand of the IPP Nagoya"
H. Bolt, A. Miyahara, T. Kuroda, O. Kaneko, Y. Kubota, Y. Oka and K. Sakurai (1987)

Available upon request to Research Information Center, Institute of Plasma Physics, Nagoya University, Nagoya 464, Japan, except for the reports noted with*.